Progress in Neuropsychopharmacology & Biological Psychiatry 122 (2023) 110690

Contents lists available at ScienceDirect

Progress in Neuropsychopharmacology & Biological Psychiatry

journal homepage: www.elsevier.com/locate/pnp

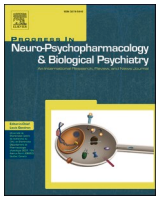

Neuromagnetic 40 Hz Auditory Steady-State Response in the left auditory cortex is related to language comprehension in children with Autism Spectrum Disorder

Vardan Arutiunian [a,*], Giorgio Arcara [b], Irina Buyanova [a], Elizaveta Davydova [c,f], Darya Pereverzeva [c], Alexander Sorokin [c,d], Svetlana Tyushkevich [c], Uliana Mamokhina [c], Kamilla Danilina [c], Olga Dragoy [a,e]

[a] Center for Language and Brain, HSE University, Moscow, Russia
[b] IRCCS San Camillo Hospital, Venice, Italy
[c] Federal Resource Center for ASD, Moscow State University of Psychology and Education, Moscow, Russia
[d] Haskins Laboratories, New Haven, CT, United States of America
[e] Institute of Linguistics, Russian Academy of Sciences, Moscow, Russia
[f] Chair of Differential Psychology and Psychophysiology, Moscow State University of Psychology and Education, Moscow, Russia

ARTICLE INFO

Keywords:
Autism Spectrum Disorder (ASD)
Magnetoencephalography (MEG)
40Hz Auditory Steady-State Response (40Hz ASSR)
Auditory gamma oscillations
Amplitude-modulated tones

ABSTRACT

Language impairment is comorbid in most children with Autism Spectrum Disorder (ASD), but its neural mechanisms are still poorly understood. Some studies hypothesize that the atypical low-level sensory perception in the auditory cortex accounts for the abnormal language development in these children. One of the potential non-invasive measures of such low-level perception can be the cortical gamma-band oscillations registered with magnetoencephalography (MEG), and 40 Hz Auditory Steady-State Response (40 Hz ASSR) is a reliable paradigm for eliciting auditory gamma response. Although there is research in children with and without ASD using 40 Hz ASSR, nothing is known about the relationship between this auditory response in children with ASD and their language abilities measured directly in formal assessment.

In the present study, we used MEG and individual brain models to investigate 40 Hz ASSR in primary-school-aged children with and without ASD. It was also used to assess how the strength of the auditory response is related to language abilities of children with ASD, their non-verbal IQ, and social functioning. A total of 40 children were included in the study.

The results demonstrated that 40 Hz ASSR was reduced in the right auditory cortex in children with ASD when comparing them to typically developing controls. Importantly, our study provides the first evidence of the association between 40 Hz ASSR in the language-dominant left auditory cortex and language comprehension in children with ASD. This link was domain-specific because the other brain-behavior correlations were non-significant.

1. Introduction

Autism Spectrum Disorder (ASD) is a heterogeneous group of neurodevelopmental conditions characterized by impaired social communication and interaction and the presence of stereotyped and repetitive behavior and restricted interests (American Psychiatric Association, 2013). Usually, most children with ASD have also a co-occurring structural language impairment, varying from severely impaired language (minimally-verbal ASD) to slightly impaired (e.g., Kjelgaard and Tager-Flusberg, 2001; Pickles et al., 2014; Tager-Flusberg and Kasari, 2013; Tager-Flusberg, 2016), but its neural mechanisms are still not clearly understood. It has been proposed that the atypical low-level sensory processing accounted for the atypical development of high-level cognitive functioning in ASD, including language (Berman et al., 2016; Matsuzaki et al., 2019; Roberts et al., 2010, 2011, 2019; Robertson and Baron-Cohen, 2017). Since a majority of individuals with autism have hyper- and/or hypo-reactivity in sensory perception, particularly the perception of auditory information (Dwyer et al., 2020;

* Corresponding author at: Center for Language and Brain, HSE University, 3 Krivokolenny pereulok, 101000 Moscow, Russia.
E-mail address: vardan.arutyunyan89@gmail.com (V. Arutiunian).

https://doi.org/10.1016/j.pnpbp.2022.110690
Received 16 May 2022; Received in revised form 6 November 2022; Accepted 29 November 2022
Available online 5 December 2022

Matsuzaki et al., 2014; Williams et al., 2021a, 2021b), this might influence language development in children with ASD.

Cortical gamma-band oscillations (30–150 Hz) registered with magnetoencephalography (MEG) and electroencephalography (EEG) can be a non-invasive measure of low-level sensory processing. The cellular studies with optogenetic manipulations have demonstrated that gamma oscillations are intimately related to the balance between neural excitation (E) and inhibition (I) (Atallah and Scanziani, 2009; Bartos et al., 2007; Ben-Ari, 2014; Dickinson et al., 2016) and are generated mostly by the gamma-aminobutyric acidergic (GABAergic) interneurons, expressing calcium-binding protein parvalbumin (PV+ inhibitory cells) (e.g., Agetsuma et al., 2018; Cardin et al., 2009; Carlén et al., 2012; Espinoza et al., 2018; Ferguson and Gao, 2018; Magueresse and Monyer, 2013). Animal models of autism, as well as MEG / EEG studies in combination with magnetic resonance spectroscopy in children with ASD, have suggested that the imbalance between E and I in the neural circuits and the dysfunction of the GABAergic inhibitory system, in general, may be one of the core pathophysiological mechanisms in this disorder (Contractor et al., 2021; Ford et al., 2019, 2020; Levin and Nelson, 2015; Rubenstein and Merzenich, 2003; Sohal and Rubenstein, 2019; Tang et al., 2021; Yizhar et al., 2011). Several studies have revealed the atypicalities of gamma response in the perception of the basic auditory and visual stimuli in children with ASD (Brown et al., 2005; Kessler et al., 2016; Seymour et al., 2020), and some authors have also proposed that the gamma-band abnormalities are the potential neural markers of ASD (Gandal et al., 2010; Rojas and Wilson, 2014).

One of the reliable paradigms to register gamma oscillations in the auditory cortex is 40 Hz Auditory Steady-State Response (40 Hz ASSR), where participants are presented with amplitude-modulated tones or a click train at a gamma frequency, usually at 40 Hz (e.g., Korczak et al., 2012; Pellegrino et al., 2019). Such stimuli activate the neuronal populations in the primary auditory cortex (or adjacent regions), which become gradually aligned in phase with the perceiving sound and reach a stable power increase at ~40 Hz during sound presentation. The advantages of the ASSR paradigm are that it is a completely passive methodology that does not require any response from participants and it has a high test-retest reliability (McFadden et al., 2014; Roach et al., 2019). Moreover, in the pediatric population, the age-related changes in the strength of 40 Hz ASSR is supposed to be associated with the maturation of GABA neurotransmission and E / I balance development (Xu et al., 2011; Williams et al., 2009; Zhang et al., 2011), indicating that inter-trial phase consistency (ITPC), a robust measure of ASSR, increases with age until early adolescence (Edgar et al., 2016; Poulsen et al., 2009). Taking all this into account, researchers asserted that ASSR is an ideal tool for investigating auditory perception in ASD (Agetsuma et al., 2018).

There are only a few MEG studies that address 40 Hz ASSR in individuals with ASD and the results of these studies are inconsistent. Wilson et al. (2007) reveal a left-hemispheric reduction of 40 Hz ASSR in children and adolescents with ASD. Seymour et al. (2020) report a bilateral reduction of 40 Hz ASSR in adolescents with ASD. Also, the reduction of ASSR has been observed in first-degree relatives of people with ASD (Rojas et al., 2011). However, other studies report no difference between children with and without ASD in this response (Edgar et al., 2016; Ono et al., 2020; Stroganova et al., 2020). Presumably, the difference in results may be explained by the duration of auditory stimulation (e.g., 500 ms in Stroganova et al. (2020) and 1500 ms in Seymour et al. (2020)), binaural vs. monaural stimulus presentation, the type of the stimuli (clicks in Stroganova et al. (2020) and amplitude-modulated tones in Edgar et al. (2016)), MEG source estimation method (e.g., Beamformer in Seymour et al. (2020) and dipole modeling in Edgar et al. (2016)), children's age, and, at last, a highly heterogeneous nature of ASD population.

Some of the previous studies have also examined the relationships between the ASSR and non-verbal IQ / severity of autistic symptoms in individuals with ASD. The results demonstrated no significant association between ASSR and non-verbal IQ (Seymour et al., 2020; Stroganova et al., 2020; Wilson et al., 2007). The link between the ASSR and autistic traits (as measured by the AQ questionnaire (Auyeung et al., 2008)) has been examined in two studies, with one reporting no significant relationship between the two (Seymour et al., 2020) and the other finding a positive relationship between ASSR amplitude and autistic traits (Stroganova et al., 2020). Although there are no studies assessing directly the relationship between 40 Hz ASSR and language abilities in children with ASD, there is only one research that is closely related to this. Roberts et al. (2021) in a large group of children with ASD ($N = 80$) using amplitude-modulated sweeps (from 10 to 100 Hz) have shown that ITPC was decreased in the ASD group compared to TD controls and, importantly, lower ITPC at a gamma-band was related to poorer language skills in children with ASD.

Another neural response that is evoked by amplitude-modulated tones (or click train) at 40 Hz is sustained Event-Related Field (ERF). Some authors have proposed that sustained ERF reflects the activity of the rate-coding neurons in the pitch-processing center (Stroganova et al., 2020) and the amplitude of sustained ERF *decreased* with age in the same cortical region that generated 40 Hz ASSR (Arutiunian et al., 2022a), so, therefore, the functional specificity and age-related changes of this response differ from 40 Hz gamma steady-state response. To the best of our knowledge, there is only one MEG study focused on sustained ERF in children with ASD (Stroganova et al., 2020). This study provides the evidence of the left-hemispheric deficit in sustained ERF discussing the possible relationship between this response and pitch processing in children with ASD. Thus, it may be beneficial to use tones with 40 Hz amplitude modulation for investigating between-group differences (ASD vs. TD) and age-related changes in both types of auditory responses.

In the present study, we used MEG to investigate 40 Hz ASSR at the source level in 8-to-14-year-old primary-school-aged children with ASD. *First,* we compared both 40 Hz ITPC and the amplitude of sustained ERF to the same periodic stimuli in children with ASD and age-matched typically-developing (TD) controls. *Second,* we examined the age-related changes in strength of both ASSR and ERF in children with ASD. *Finally,* we assessed the relationships between 40 Hz ITPC / ERF and behavioral measures (non-verbal IQ, the severity of autistic traits, and language abilities) in children with ASD. Although the previous studies have examined how ASSR was associated with non-verbal IQ and the severity of autistic symptoms, to the best of our knowledge, this is the first study assessing the relationship between ASSR and the language abilities of children with ASD measured directly, i.e., with a standardized language assessment tool.

2. Methods

2.1. Participants

A total of 40 children were included into the study: 20 children with ASD (5 girls, age range 8.02–14.01 years, $M_{age} = 10.03$, $SD = 1.7$) and 20 age-matched TD children (9 girls, age range 7.02–12.03 years, $M_{age} = 9.11$, $SD = 1.3$). Children with ASD were recruited from the Federal Resource Center for Organization of Comprehensive Support to Children with Autism Spectrum Disorders (Moscow, Russia) and TD children were recruited from public schools in Moscow.

The study was approved by the ethics committee of Moscow State University of Psychology and Education (for ASD group) and the HSE University Committee on Interuniversity Surveys and Ethical Assessment of Empirical Research (for TD group), and was conducted following the ethical principles regarding human experimentation (the Declaration of Helsinki). All children and their parents provided the verbal assent to participate in the study and were informed that they can withdraw from the study at any time during the experiment. A written consent form was obtained from a parent of each child.

2.2. Clinical and behavioral assessment

The diagnosis of all children with ASD based on the criteria of the International Classification of Diseases – 10 (World Health Organization, 2016), and 18 out of 20 children were also assessed by a licensed psychiatrist with Autism Diagnosis Observation Schedule – Second Edition, ADOS-2 (Lord et al., 2012). Additionally, to confirm the validity of the diagnosis, the parents of both groups of children were asked to complete the Russian translation of the Autism Spectrum Quotient: Children's Version, AQ (Auyeung et al., 2008). The criteria of exclusion from the study were comorbid neurological disorders (e.g., epilepsy) and the presence of a known chromosomal syndrome (e.g., Rett syndrome, Fragile X syndrome). The information of medication status of children was not available.

The non-verbal IQ of children with ASD has been evaluated with the Kaufman Assessment Battery for Children K-ABC II, NVI index (Kaufman and Kaufman, 2004), or the Wechsler Intelligence Scale for Children – Third Edition, performance IQ score (Wechsler, 1991); the non-verbal intelligence of TD children was screened with the Raven's Colored Progressive Matrices (Raven, 2000). Language abilities of both groups were measured with the Russian Child Language Assessment Battery (Arutiunian et al., 2022b), a standardized test for assessment of phonology, vocabulary, morphosyntax, and discourse in both production and comprehension; mean language score (MLS) across all subtests, as well as language production score (LPS) and language comprehension score (LCS) were calculated for each child.

TD children did not have a history of psychiatric and/or neurodevelopmental disorders and, according to language and non-verbal IQ testing, all of them were within the normal range. All children from both groups had normal hearing and normal or corrected-to-normal vision, based on both parental reports and formal assessment.

Demographic information for ASD and TD groups of children is presented in Table 1.

2.3. Auditory stimuli

The auditory stimuli were tones with 40 Hz amplitude modulation with a 6 ms fade-in and fade-out periods, were normalized so to prevent clipping (Fig. 1), and were taken from the previous study (Arutiunian et al., 2022a). They were generated with in-home MATLAB code according to the formula:

$$A = sin\,(2\pi f_c t) \times (1 + m \times cos(2\pi f_m t))$$

where A is the amplitude, f_c is the carrier frequency, set to 1000, m is the modulation depth, set to 1, f_m is the frequency of modulation, set to 40, t is the vector of time points for 1 s of stimulus at a sampling rate of 44,100 Hz.

2.4. Procedure

The experiment was programmed and run with the PsychoPy software, version 1.90.2 with audio library 'pyo' (Peirce, 2007). The presentation of auditory stimuli (each with 1000 ms duration) was binaural, and the intervals between them were fixed at 2000 ms. Overall, 90 amplitude-modulated tones were presented during one ~5 min block. Stimuli were delivered via plastic ear tubes with foam tips inserted into the ear canals, and the intensity level was set at 83.7 dB sound pressure level. Together with the triggers sent by PsychoPy to the MEG acquisition system, an analog channel of the MEG system recorded the onset of the actual sound sent to the ear tubes. The signal from the analog channel was used to adjust the trigger positions, compensating for the delay between sound presentation by the software and its actual arrival to the ears. In order to reduce eye movements, the children were asked to look at the fixation cross on the screen in front of them during the experiment (see Fig. 1a).

2.5. Structural magnetic resonance imaging (MRI) acquisition

The high-resolution whole-brain structural MRIs were acquired with a 1.5 T Siemens Avanto scanner with the following parameters: repetition time = 1900 ms, echo time = 3.37 ms, flip angle = 15°, matrix size = 256 × 256 × 176, voxel size = 1.0 × 1.0 × 1.0 mm^3. The MRI segmentation and reconstruction of the cortical surface from the individual MRIs were performed with the FreeSurfer software (Dale et al., 1999). The surface was then imported to the Brainstorm toolbox (Tadel et al., 2011) and down-sampled to 15,000 vertices for each participant. MRI – MEG co-registration was performed with the Brainstorm toolbox based on the six reference points (left and right pre-auricular points, nasion, anterior and posterior commissure, and interhemispheric point) and the additional digitized head points ($N = \sim 150$).

T1 MRIs were obtained for all TD children and for 15 out of 20 children with ASD. Five children with ASD had severe behavioral issues, so that they could not lie still in the MRI scanner. For these children, we used the template anatomy (MRI: ICBM152) but applied the special warping procedure implemented in Brainstorm. This procedure allowed for building the pseudo-individual brains based on the head points

Table 1
The demographic information for ASD and TD groups of children, $M \pm SD$ (range).

Characteristics	Group		t	p	*Cohen's d*
	ASD ($N = 20$)	TD ($N = 20$)			
Age in years	10.03 ± 1.7 (8.02–14.01)	09.11 ± 1.3 (7.02–12.03)	0.70	0.48	0.22
Mean language score[1]	0.75 ± 0.23 (0.20–0.93)	0.95 ± 0.02 (0.91–0.99)	−4.04	<0.001***	−1.27
Language production	0.76 ± 0.24 (0.12–0.95)	0.96 ± 0.02 (0.93–0.99)	−3.66	0.001**	−1.15
Language comprehension	0.73 ± 0.24 (0.24–0.94)	0.95 ± 0.03 (0.88–1.00)	−4.07	<0.001***	−1.28
AQ total	83.6 ± 18.8 (45–120)	50.2 ± 14.2 (25–83)	6.23	<0.001***	2.00
AQ social skills	15.9 ± 6.0 (4–25)	7.6 ± 3.0 (3–12)	5.50	<0.001***	1.73
AQ attention switching	16.2 ± 4.0 (11–23)	12.3 ± 3.0 (6–20)	3.39	0.001**	1.07
AQ attention to details	14.9 ± 4.9 (4–23)	12.8 ± 4.9 (3–23)	1.37	0.17	0.43
AQ communication	21.1 ± 4.2 (9–29)	8.6 ± 4.7 (1–18)	8.94	<0.001***	2.82
AQ imagination	15.4 ± 6.4 (2–27)	8.9 ± 3.1 (4–14)	4.07	<0.001***	1.28
Non-verbal IQ: K-ABC ($N_{children} = 15$) or WISC III score ($N_{children} = 5$)	85.4 ± 17.9 (41–118)	–	–	–	–
Non-verbal IQ: Raven's matrices score ($N_{children} = 20$)	–	31.8 ± 2.7 (23–36)	–	–	–
ADOS, raw score					
Module 1 ($N_{children} = 1$)	12	NA	–	–	–
Module 2 ($N_{children} = 5$)	16.2 ± 4.96 (8–20)	NA	–	–	–
Module 3 ($N_{children} = 12$)	10.5 ± 1.98 (8–14)	NA	–	–	–

Note: [1]Mean language score (as well as language production and language comprehension scores) is a standard average score (from 0 to 1) across all subtests of the Russian Child Language Assessment Battery (see Arutiunian et al., 2022b). We run t-tests to compare the characteristics of ASD and TD groups of children. The significance is labeled with $*p < 0.05$, $**p < 0.01$, $***p < 0.001$.

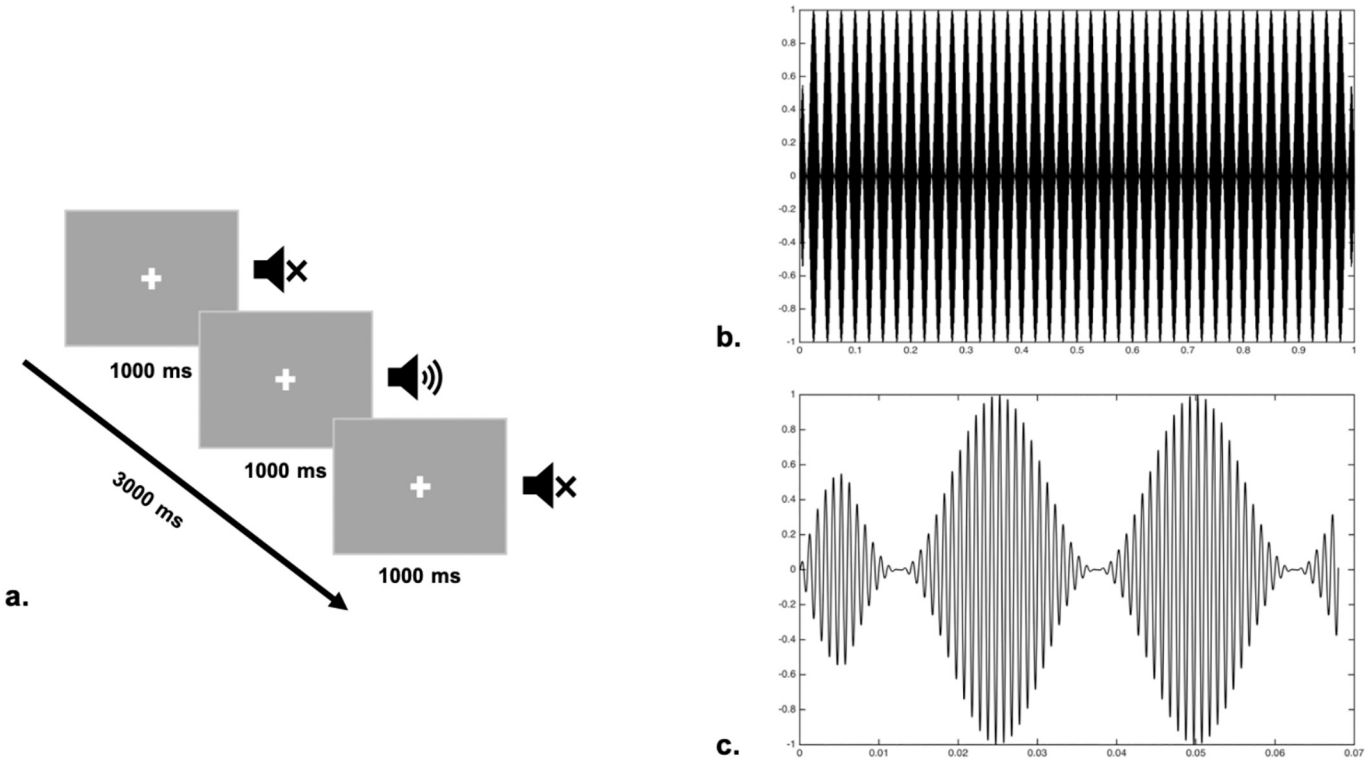

Fig. 1. The presentation of stimulus: (a) The structure of a trial; (b) 40 Hz amplitude-modulated tone (the duration is 1000 ms); (c) The first 70 ms of the stimulus (for visualization purpose).

digitized before the MEG data collection and represented the real head shape of each child.

2.6. MEG data collection and pre-processing

MEG was recorded in a sitting position in a magnetically shielded room with a whole-head 306-channel MEG (Vectorview, Elekta Neuromag), comprising 204 orthogonal planar gradiometers and 102 magnetometers. The position of children's head within the MEG helmet was monitored every 4 ms during the experiment via four head position indicator (HPI) coils digitized together with fiducial points using 3D digitizer 'Fastrak' (Polhemus). We applied the temporal signal space separation (Taulu and Simola, 2006) and movement compensation procedures implemented in MaxFilter software (Elekta Neuromag) to remove external interference signals generated outside the brain and to compensate for head movements. An electrooculogram (EOG) was recorded using four electrodes placed above and below the left eye (to detect the blinks) as well as at the left and right outer canthi (to detect horizontal eye movements). An electrocardiography (ECG) was monitored with ECG electrodes to compensate for cardiac artifacts.

MEG was recorded at 1000 Hz sampling rate and filtered off-line with a band-pass filter of 0.1–330 Hz for the time-frequency (TF) analysis and 0.1–45 Hz for the event-related field (ERF) analysis. A notch filter of 50 Hz was applied to reduce powerline noise. The artifacts (heartbeats and eye movements) were cleaned with the EEGLAB's (Delorme and Makeig, 2004) Independent Component Analysis (ICA) implemented in Brainstorm.

The cleaned MEG data were cut in 3000 ms epochs, ranging from −1500 ms to 1500 ms, and DC offset correction from −100 ms to −2 ms was applied. Epochs were inspected visually and those affected by the muscular artifacts were manually rejected. The number of artifact-free epochs did not differ between groups of children: *TD group,* $M_{\text{number}} = 84$, $SD = 3.30$, range 77–87; *ASD group,* $M_{\text{number}} = 84$, $SD = 3.85$, range 75–87; $t(37.13) = 0.17$, $p = 0.86$.

2.7. MEG source estimation

We used only gradiometers for the analysis because of the current debates over mixing both magnetometers and gradiometers, which have different levels of noise (see Seymour et al., 2020). The individual head models were built with the 'Overlapping spheres' method (Huang et al., 1999), and the inverse problem was solved with the depth-weighted linear L2-minimum norm estimate method (Lin et al., 2006), with the dipole orientation constrained to be normal to the cortical surface. The regularization parameter ($\lambda = 0.33$) was used when computing the inverse operator (Hämäläinen and Ilmoniemi, 1994). A common imaging kernel was computed and then applied to obtain single epoch cortical reconstructions. A noise covariance was calculated from a 2 min empty room recording, taken after each participant's recording session. In order to provide the comparison between subjects, the individual MNEs were projected to the 'MRI: ICBM152' template brain.

According to the previous findings (Farahani et al., 2021), cortical generators of ASSR are spread over the auditory regions in both hemispheres. In order to estimate the sources of ASSR, we selected the following regions of interest (ROIs): transverse temporal gyrus, transverse temporal sulcus, planum temporale of the superior temporal gyrus, lateral superior temporal gyrus, superior temporal sulcus, planum polar of the superior temporal gyrus, and inferior part of the circular sulcus of the insula in the left and right auditory cortices, based on the Destrieux parcellation cortical atlas (Destrieux et al., 2010).

The TF analysis at the source level was performed with the Morlet wavelets (central frequency = 40 Hz, time resolution = 0.3 s). We calculated 40 Hz Inter-Trial Phase Consistency (ITPC), which computes the phase consistency across the trials as follows:

$$ITPC = \left| n^{-1} \sum_{r=1}^{n} e^{ik} tr \right|$$

where n is the number of trials, e^{ik} is the complex polar representation of phase angel k on trial r, at the timepoint t. The phases were estimated

from the Morlet wavelet coefficients. ITPC can take values from 0.0 to 1.0, whereby higher values indicate higher consistency of phases across the trials (Nash-Kille and Sharma, 2014). TF maps were normalized with an Event-Related Perturbation (Event-Related Synchronization / Event-Related Desynchronization) approach considering a time window between −500 ms and − 200 ms as a baseline, evaluating the deviation from the mean over the baseline, according to the formula: (x – mean)/ mean × 100. We analyzed ITPC because it was revealed that it is more sensitive to age-related changes in the 40 Hz ASSR than power (Edgar et al., 2016) and also ITPC is a more reliable measure in comparison to total power in the same frequency range (Tan et al., 2015).

The normalized ITPC values were averaged in the 39–41 Hz frequency range in the interval from 200 ms to 900 ms after stimulus onset ('40 Hz ITPC'). This time interval was chosen based on the previous study which showed that the auditory cortex reaches a steady state after about 200 ms of 40 Hz entrainment (Arutiunian et al., 2022a). To estimate the cortical sources of ASSR for each child, we estimated MNI coordinates of 30 vertices with the highest 40 Hz ITPC values in the defined ROIs (15 vertices per hemisphere), and for the further analysis extracted 40 Hz ITPC values averaged over these 15 vertices in the time interval between 200 ms and 900 ms in each hemisphere for each child. We have chosen such an approach in order to take into account the individual variability of responses within the 'core auditory area' (defined ROIs), which provides a more precise source estimation as it has been shown in the previous studies (Arutiunian et al., 2022a; Stroganova et al., 2020).

For the ERF analysis, the signal was averaged over epochs, and the individual time course was calculated for each of 15,000 vertices. Then the cortical map was normalized with a *z*-score, using the pre-stimulus baseline of −100 ms to −2 ms. For each child, *z*-score normalized absolute values were averaged in the time interval between 200 ms and 1000 ms and were extracted for the same regions as for 40 Hz ITPC in the left and right auditory ROIs. Such a window of interest for the ERF analysis was chosen because the 'sustained' component of the evoked response begins at around 200 ms and stays stable during auditory presentation, which has been shown in the previous study (Arutiunian et al., 2022a). A special smoothing function based on the Gaussian smoothing (full width at half maximum, FWHM = 3 mm) was applied.

2.8. Statistical analysis

Linear models with and without mixed effects, interactions and nested contrasts were used to estimate between-group differences in ASSR and ERF responses, as well as relationships between neural responses (the structures of the models will be provided further). Additionally, we used Pearson's correlations to analyze the age-related changes in these neural responses and the associations between ASSR / ERF and behavioral measures (language abilities, non-verbal IQ, severity of autism) in children with ASD.

Numeric variables in all models were centered to avoid multicollinearity. All models were estimated in R (R Core Team, 2019) with the *lme4* (Bates et al., 2015) package. Correlation analysis was done with *Hmisc* (Harrell Jr. and Dupont, 2020) and *cocor* (Diedenhofen and Musch, 2015) packages. The tables for model outcomes were built with the *sjPlot* package (Lüdecke, 2020), and the data were plotted with *ggplot2* (Wickham, 2016).

3. Results

3.1. Participants' characteristics

3.1.1. The severity of autistic traits

According to the total AQ score (the parents' questionnaire), the severity of autistic symptoms was significantly higher in children with ASD: $M_{ASD} = 83.6$ ($SD = 18.8$) vs. $M_{TD} = 50.2$ ($SD = 14.2$), $t(35.4) = 6.23$, $p < 0.001$. Between-group comparisons of the AQ 'scales' associated with autism and broader phenotype also revealed significant differences in four out of five scales (see Table 1). Therefore, the analysis showed that the AQ scores were higher in the ASD group on each 'scale', excluding the scale assessing the attention to details.

3.1.2. Language abilities

There were also significant differences between groups of children in their language abilities: *MLS,* $M_{ASD} = 0.75$ ($SD = 0.23$) vs. $M_{TD} = 0.95$ ($SD = 0.02$), $t(19.37) = -4.04$, $p < 0.001$; *LPS,* $M_{ASD} = 0.76$ ($SD = 0.24$) vs. $M_{TD} = 0.96$ ($SD = 0.02$), $t(19.26) = -3.66$, $p = 0.001$; *LCS,* $M_{ASD} = 0.73$ ($SD = 0.24$) vs. $M_{TD} = 0.95$ ($SD = 0.03$), $t(19.66) = -4.07$, $p < 0.001$. This demonstrated that children with ASD had language impairment in production and comprehension (see Table 1).

In general, the group of children with ASD was highly heterogeneous, and there was a variability in non-verbal IQ (from very low, IQ = 40, to normal, IQ = 118) and language abilities (from severely impaired to normal). To explore this variability, we performed Pearson's correlation analysis among behavioral measures (MLS, non-verbal IQ, and ADOS calibrated severity score). There was a significant relationship between IQ and MLS, $R = 0.61$, $p = 0.004$, indicating that lower non-verbal cognition was associated with a lower language score. The correlations between ADOS calibrated severity score and non-verbal IQ as well as MLS were non-significant, and there were no significant relationships between children's age and non-verbal IQ, ADOS total score, and MLS.

3.2. Sensor-level plots of auditory response (raw data) in children with and without ASD

To explore whether the obligatory auditory transient components (M50 and M100) and sustained ERF are presented in children with and without ASD, we calculated grand average raw-data sensor-level plots (Fig. 2). The visualization of the raw data demonstrates a clear presence of M50 component at around 60 ms, followed by M100 component at around 110 ms, as well as the sustained ERF after about 200 ms from the stimulus onset in both groups of children. The corresponding source activation at these timepoints shows the highest *z*-score values in the primary auditory cortex and in the vicinity of this region in the left and right hemispheres.

3.3. Source estimation of 40 Hz ASSR in the auditory cortex

To estimate the sources of 40 Hz ASSR in the left and right auditory cortices as well as to compare the localization of sources between groups of children, the normalized ITPC was calculated in the 200–900 ms time interval after stimulus onset, and MNI coordinates for 15 vertices in each ROI with the highest 40 Hz ITPC-values (separately for each participant) were obtained. The grand average MNI coordinates for ASSR is presented in Table 2 for both ASD and TD groups of children.

These results are in line with the previous studies, indicating that the sources of 40 Hz ASSR are located in the primary auditory cortex or in the vicinity of this region (Keceli et al., 2015; Stroganova et al., 2020) in both groups of children. Fig. 3 visualizes both individual and grand average MNI coordinates of the response in both hemispheres in children with and without ASD.

To test whether there are between-group differences (ASD vs. TD) in the location of ASSR, we performed MANOVA to compare MNI coordinates in each hemisphere. The results showed no significant difference in either X, Y or Z coordinates: *left X,* $F = 0.64$, $p = 0.42$; *left Y,* $F = 0.06$, $p = 0.80$; *left Z,* $F = 0.002$, $p = 0.96$; *right X,* $F = 0.56$, $p = 0.45$; *right Y,* $F = 1.65$, $p = 0.20$; *right Z,* $F = 0.11$, $p = 0.73$. Thus, we did not find the evidence for the differences in the topography of cortical sources of ASSR between children with and without ASD in any hemisphere.

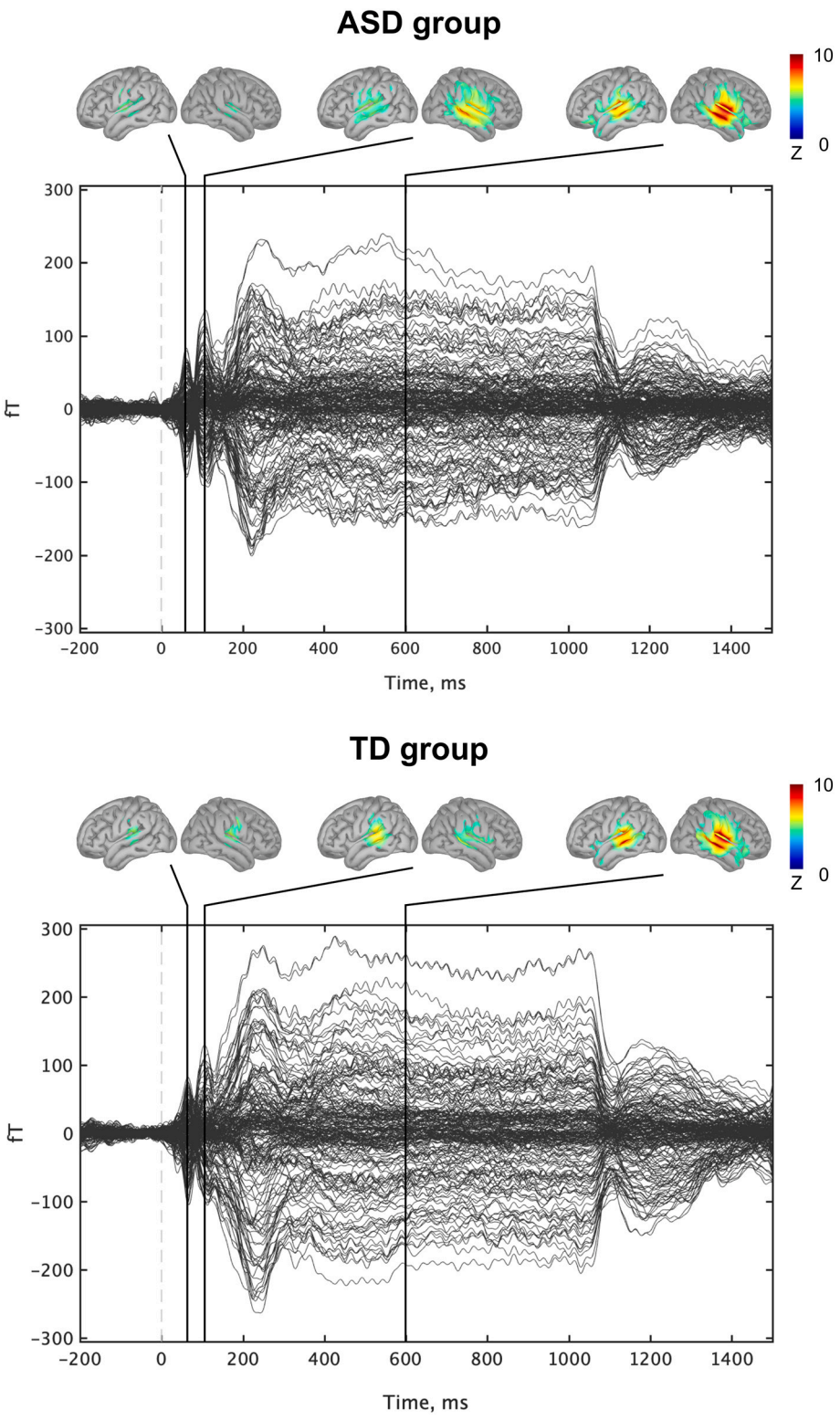

Fig. 2. The grand average sensor-level 'butterfly' plots of 204 gradiometers for ASD and TD groups of children; the black lines correspond to the first obligatory transient auditory components in MEG (M50 and M100) and sustained part of Event-Related Fields; the top panels show the distribution of cortical activity at these timepoints.

3.4. The comparison of 40 Hz ASSR and ERF between children with and without ASD

In order to compare ASD and TD groups of children in 40 Hz ITPC, we fitted a linear mixed-effects model including the main effects of group (ASD vs. TD), hemisphere (left vs. right), and group × hemisphere interaction as fixed effects, and participants as a random intercept (also see Supplementary materials with additional results on the power of 40 Hz ASSR as well as the reliability of each MEG-derived indices). The structure of the model was as follows: *lmer(ITPC ~ 1 + Group + Hemisphere + Group × Hemisphere + (1 | ID), data = data, control = lmerControl(optimizer = "bobyqa"))*. The results showed a significant main

Table 2
Grand average MNI coordinates for 40 Hz Auditory Steady-State Response for ASD and TD groups of children.

Group	Left auditory ROI			Right auditory ROI		
	Coordinate	Mean	SD	Coordinate	Mean	SD
ASD	X	−50.65	7.67	X	54.59	5.44
	Y	−21.57	15.30	Y	−21.25	8.81
	Z	6.73	12.70	Z	9.35	9.59
TD	X	−48.72	7.52	X	53.30	5.45
	Y	−22.73	14.05	Y	−24.43	6.72
	Z	6.91	11.76	Z	10.24	6.66

effect of hemisphere, β = −126.42, SE = 26.92, t = −4.69, p < 0.0001, and also a significant group × hemisphere interaction, β = 109.25, SE = 26.92, t = 4.06, p = 0.0002. The main effect of group was non-significant, β = −33.70, SE = 42.31, t = −0.79, p = 0.43. To analyze between-group differences in 40 Hz ASSR in each hemisphere separately, we fitted a linear mixed-effects model including the main effect of hemisphere (left vs. right, intercept corresponding to the left), the effect of group nested within the left and right hemispheres separately as fixed effects, and participants as a random intercept, according to the formula: *lmer(ITPC ~ 1 + Hemisphere / Group + (1 | ID), data = data, control = lmerControl(optimizer = "bobyqa"))*.

The results revealed a reduction of 40 Hz ITPC in the right hemisphere in children with ASD, but no difference between groups in the left hemisphere: *left auditory ROI,* M_{ASD} = 481.88 (*SD* = 364.28) vs. M_{TD} = 330.78 (*SD* = 192.68), β = −151.09, SE = 100.30, t = −1.51, p = 0.132; *right auditory ROI,* M_{ASD} = 516.21 (*SD* = 270.25) vs. M_{TD} = 802.12 (*SD* = 399.45), β = 285.91, SE = 100.30, t = 2.85, p = 0.005 (Table 3, Figs. 4a – 4c).

To compare the sustained part of ERF in ASD and TD groups of children, we fitted a linear model including the main effects of group (ASD vs. TD), hemisphere (left vs. right), and group × hemisphere interaction. The structure of the model was as follows: *lmer(ERF ~ 1 + Group + Hemisphere + Group × Hemisphere, data = data)*. The results showed a significant main effect of hemisphere, β = −1.53, SE = 0.62, t = −2.46, p = 0.01, but no main effect of group, β = −0.45, SE = 0.62, t = −0.73, p = 0.46, or group × hemisphere interaction, β = −0.14, SE = 0.62, t = −4.23, p = 0.81 were found. To compare a sustained part of ERF in each hemisphere separately between children with and without ASD, we fitted a linear model including a main effect of hemisphere (left vs. right, intercept corresponding to right) and the effect of group nested within the left and right hemispheres separately, according to the formula: *lm(ERF ~ 1 + Hemisphere / Group, data = data)*.

The results showed no difference in the amplitude of sustained ERF between groups of children (Table 4, Figs. 4d – 4f). In order to explore a possible between-group difference in ERF at a specific time window, we divided the sustained part of ERF timecourse into four equal windows with 200 ms duration and provided window-by-window comparisons between ASD and TD groups of children. Two-sample t-tests also revealed no difference between groups in any time windows: *left auditory ROI,* 200–400 ms, $t(37)$ = −1.11, p = 0.27; 400–600 ms, $t(35)$ = −0.85, p = 0.39; 600–800 ms, $t(37)$ = −0.26, p = 0.79; 800–1000 ms, $t(35)$ = −0.40, p = 0.68; *right auditory ROI,* 200–400 ms, $t(37)$ = −0.64, p = 0.52; 400–600 ms, $t(32)$ = −0.47, p = 0.63; 600–800 ms, $t(30)$ = −0.10, p = 0.92; 800–1000 ms, $t(35)$ = −0.02, p = 0.97.

3.5. The hemispheric dominance of 40 Hz ASSR and the age-related changes of ASSR and ERF responses in children with and without ASD

Based on the hypothesis of atypical development of auditory cortex in children with ASD (Roberts et al., 2010, 2019), we analyzed how both types of neural responses (40 Hz ASSR and ERF) are related to each other in the left and right hemispheres in ASD and TD groups of children separately (see Roberts et al. (2021)). We fitted individual linear mixed-effects models including the main effects of hemisphere (left vs. right), source amplitude (ERF), and hemisphere × source amplitude interaction as fixed effects, and participants as a random intercept, based on the formula: *lmer(ITPC ~ 1 + Hemisphere + Amplitude + Hemisphere × Amplitude + (1 | ID), data = data, control = lmerControl(optimizer = "bobyqa"))*. In TD group, there were significant main effects of hemisphere, β = −576.77, SE = 81.93, t = −7.04, p < 0.00001, source amplitude, β = −22.66, SE = 6.83, t = −3.31, p = 0.002, and a significant hemisphere × source amplitude interaction, β = 30.75, SE = 7.33, t = 4.19, p = 0.0002. The analysis of nested contrasts of ERF in each hemisphere (*lmer(ITPC ~ 1 + Hemisphere / ERF + (1 | ID), data = data, control = lmerControl(optimizer = "bobyqa"))*) revealed a right hemispheric dominance of 40 Hz ITPC, M_{Left} = 330.78 (*SD* = 192.68) vs. M_{Right} = 802.12 (*SD* = 399.45), β = −576.77, SE = 81.93, t = −7.04, p < 0.0001 (Table 5, Fig. 5), and a significant relationship between 40 Hz ITPC and the source amplitude in the right auditory ROI, β = −53.41, SE = 11.24, t = −4.75, p < 0.0001, replicating the previous findings on a larger group of TD children (Arutiunian et al., 2022a). In ASD group, there were significant main effects of hemisphere, β = −217.60, SE = 76.76, t = −2.83, p = 0.008, source amplitude, β = 27.24, SE = 7.90, t = 3.44, p = 0.0001, and a significant hemisphere × source amplitude interaction, β = 26.86, SE = 7.75, t = 3.46, p = 0.001. The analysis of nested effects demonstrated that, as in TD children, there was a right hemispheric dominance of 40 Hz ITPC, M_{Left} = 481.88 (*SD* = 364.28) vs. M_{Right} = 516.21 (*SD* = 270.25), β = −217.61, SE = 76.77, t = −2.83, p = 0.008 (see Table 5, Fig. 5). Therefore, although children with ASD had a reduced 40 Hz ITPC in the right auditory ROI, the pattern and asymmetry of response were similar to those of TD group.

In comparison to TD group, children with ASD had the atypical relationship between 40 Hz ASSR and ERF responses. In TD children, there was a negative association between 40 Hz ITPC and the amplitude of ERF response, so that the higher ITPC was associated with lower source amplitude in the right auditory ROI. By contrast, there was no such effect in the group of children with ASD. Moreover, there was an atypical significant relationship between 40 Hz ITPC and the amplitude of ERF response in the left auditory ROI, indicating that the *higher* ITPC was related to the *higher* source amplitude: β = 54.11, SE = 13.06, t = 4.14, p < 0.001.

To investigate the age-related changes in neural responses, we performed Pearson's correlation analysis in children with and without ASD in both hemispheres. In TD group, there was a significant association between 40 Hz ITPC and age in the right auditory cortex, indicating that the lower strength was related to younger age, *right auditory ROI,* R = 0.75, Bonferroni-corrected p = 0.0004, 95% C.I. [0.46, 0.89]; *left auditory ROI,* R = 0.52, Bonferroni-corrected p = 0.08, 95% C.I. [0.10, 0.78]. In ASD group, there were no any significant relationships between 40 Hz ITPC and age, *left auditory ROI,* R = 0.005, Bonferroni-corrected p = 1.00, 95% C.I. [−0.43, 0.44]; *right auditory ROI,* R = 0.33, Bonferroni-corrected p = 0.64, 95% C.I. [−0.13, 0.67]. A statistical comparison of two correlations (TD vs. ASD in the right hemisphere) showed a significant difference between groups, z = −1.98, p = 0.04. The results of TD group are in line with the previous findings which showed a monotonic age-related increase of 40 Hz ITPC in the right auditory cortex (Arutiunian et al., 2022a; Cho et al., 2015; Edgar et al., 2016; Seymour et al., 2020; Stroganova et al., 2020). This indicated, therefore, that children with ASD had not only a reduced 40 Hz ITPC in the right auditory ROI, but also the atypical developmental state of this response. The relationship between the amplitude of sustained ERF and the age was not significant after correction for multiple comparisons in any group in both hemispheres: TD group, *left auditory ROI,* R = −0.13, Bonferroni-corrected p = 1.00, 95% C.I. [−0.54, 0.33]; *right auditory ROI,* R = −0.50, Bonferroni-corrected p = 0.08, 95% C.I. [−0.77, −0.07]; ASD group, *left auditory ROI,* R = −0.36, Bonferroni-corrected p = 0.44, 95% C.I. [−0.69, 0.09]; *right auditory ROI,* R = −0.21, Bonferroni-corrected p = 1.00, 95% C.I. [−0.59, 0.25].

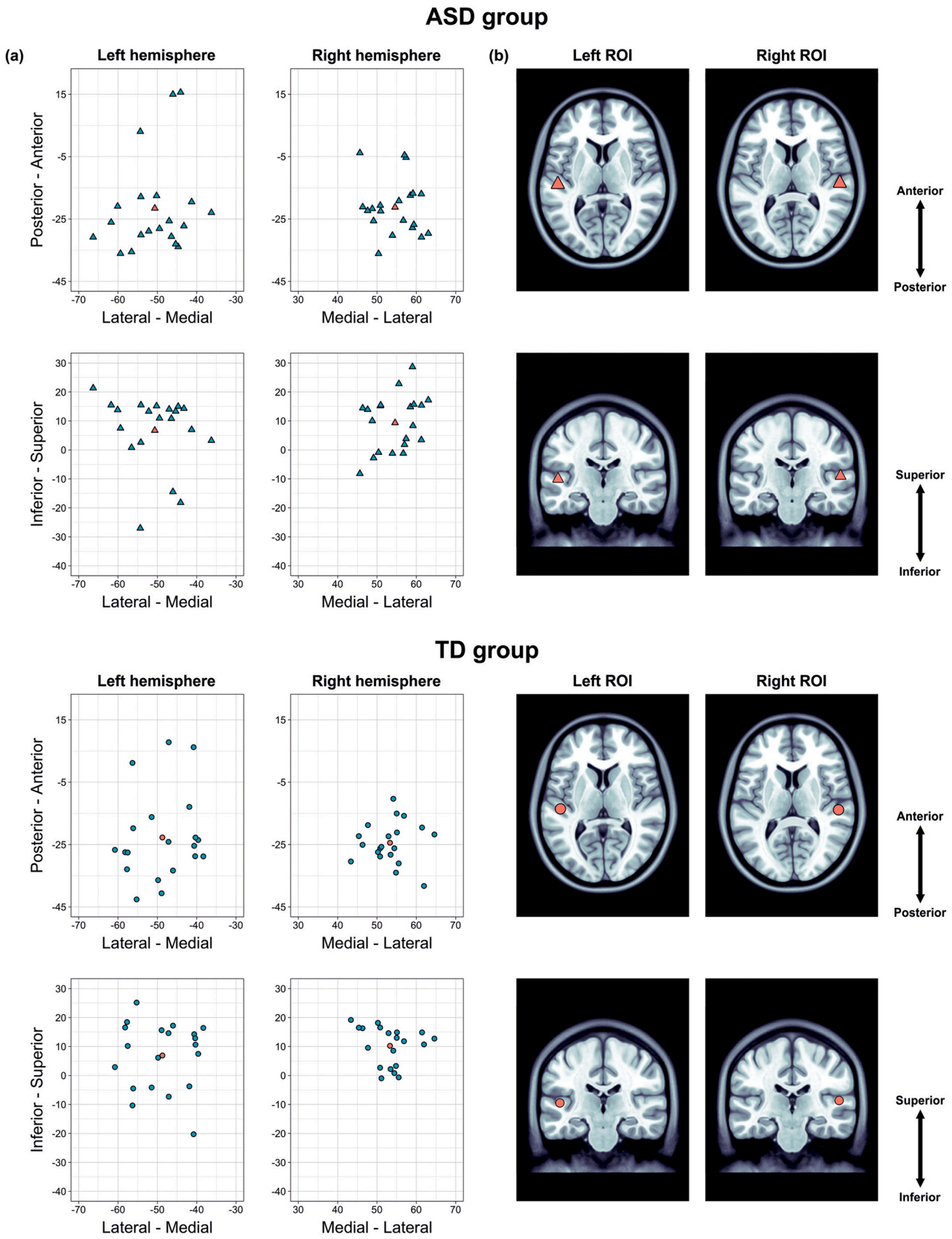

Fig. 3. The localization of 40 Hz Auditory Steady-State Response (ASSR) in MNI space for ASD and TD groups of children: (a) MNI coordinates of 40 Hz ASSR in the left and right hemispheres: blue dots / triangles represent the individual MNI coordinates of each child, red dots / triangles represent the grand average MNI coordinates; (b) Grand average MNI coordinates of 40 Hz ASSR in axial and coronal directions for both groups of children. (For interpretation of the references to colour in this figure legend, the reader is referred to the web version of this article.)

Table 3
The comparison of 40 Hz Auditory Steady-State Response between ASD and TD groups of children.

	40 Hz Inter-Trial phase consistency			
Predictors	Estimate	Standard error	*t*	*p*
(Intercept)	−33.70	59.84	−0.56	0.573
Hemisphere_Left	−17.17	38.07	−0.45	0.652
Hemisphere_Left:TD_group	−151.09	100.30	−1.51	0.132
Hemisphere_Right:TD_group	285.91	100.30	2.85	**0.005****
Random Effects				
σ^2	57,985.38			
$\tau_{00\ ID}$	42,622.48			
ICC	0.42			
$N_{\ ID}$	40			
Observations	80			
Marginal R^2 / Conditional R^2	0.226 / 0.554			

3.6. The association between brain responses and behavioral measures in children with ASD

In order to investigate how both types of auditory responses (40 Hz ASSR and ERF) in children with ASD are related to behavioral measures (language score, non-verbal IQ, and the severity of autistic symptoms), we run Pearson's correlations.

3.6.1. The relationships between 40 Hz ASSR and MLS, IQ, AQ scores

In the right auditory ROI, the analysis revealed no significant associations between 40 Hz ITPC and any behavioral measures. In the left auditory ROI, there were no significant relationships between 40 Hz ITPC and IQ as well as AQ scores, but there was a significant effect of MLS: $R = 0.57$, Bonferroni-corrected $p = 0.04$, 95% C.I. [0.17, 0.80], indicating that the lower 40 Hz ITPC in the left hemisphere was related to more impaired language abilities of children with ASD (Fig. 6a). Additionally, to test whether language production and language comprehension scores had different effects, we correlated LPS and LCS with 40 Hz ITPC separately. The results revealed no significant association between LPS and 40 Hz ITPC, $R = 0.42$, $p = 0.06$, 95% C.I. [−0.02, 0.72], but there was a significant relationship between LCS and 40 Hz ITPC, $R = 0.60$, $p = 0.005$, 95% C.I. [0.21, 0.82]. This indicated that 40 Hz ASSR in the left auditory ROI was related to language comprehension in children with ASD.

3.6.2. The relationships between sustained ERF response and MLS, IQ, AQ scores

There were no significant relationships between the amplitude of ERF and behavioral measures in either left or right auditory ROIs (Fig. 6b).

4. Discussion

In the present study, we used MEG to investigate 40 Hz ASSR and sustained ERF responses to the same amplitude-modulated tones at the source level in children with and without ASD and also to assess the relationships between these responses and behavioral measures (language abilities, non-verbal IQ, and the severity of autistic symptoms) in children with ASD. The novelty of the study was to highlight how 40 Hz ASSR is related to the language abilities (both production and comprehension) of children with ASD measured directly, i.e., with a standardized language assessment tool.

4.1. Source estimation of 40 Hz ASSR in children with and without ASD

We localized sources for 40 Hz ASSR in TD children and children with ASD and, in accordance with the previous studies, the neural generators of the response were in the primary auditory cortex (A1) and adjacent regions in the left and right hemispheres in both groups of children (Edgar et al., 2016; Seymour et al., 2020; Stroganova et al., 2020). The direct between-group comparison of MNI coordinates did not reveal significant differences in either X, Y, or Z in any hemisphere, indicating that the topology of ASSR was similar in children with and without ASD. This is in line with Stroganova et al. (2020) who also compared MNI coordinates between typically developing children and children with autism.

In contrast to Edgar and colleagues' MEG study (Edgar et al., 2016) with a similar age-range group, we could detect a clear 40 Hz ASSR in all children from both groups, whereas in their study, 40 Hz ASSR was not observed in the majority of children. The authors concluded that the difficulties in measuring this response in children make this paradigm nonoptimal for assessing steady-state 40 Hz auditory gamma response in the pediatric population (Edgar et al., 2016). However, in a more recent MEG study by Stroganova et al. (2020), 40 Hz ASSR was also detected in most children with and without ASD. The authors hypothesized that contrary to Edgar et al. (2016) study, they could detect 40 Hz ASSR in most of the children from their sample owing to the methodological differences, such as stimulus presentation (monaural instead of binaural), the type of the auditory stimuli (clicks instead of the amplitude-modulated tones), and the source estimation methods (sLORETA instead of single dipole modeling). Our findings contribute to this discussion because we detected 40 Hz ASSR in both groups of children using the same paradigm as in Edgar et al. (2016) study: amplitude-modulated tones presented binaurally. It means that stimulus presentation and type did not account for the possibility to detect the response, whereas the source estimation method plays a significant role in it. Given the individual variability in the location of 40 Hz ASSR even in adults (Farahani et al., 2021), we suggest that for precise source estimation we need to take into consideration the number of anatomical ROIs in the 'core auditory area' (see Methods) to explore inter-individual differences across children (also see the discussion on the individual variability in the topology of 40 Hz ASSR in the recent study (Arutiunian et al., 2022a)).

4.2. The comparison of 40 Hz ASSR and sustained ERF in children with and without ASD

Similarly to the previous studies in children and adolescents with ASD (Seymour et al., 2020; Wilson et al., 2007) and their first-degree relatives (Rojas et al., 2008, 2011), we showed a reduction in the strength of 40 Hz steady-state auditory gamma response in our ASD sample. However, all these findings disagree on the laterality of the pathological decrease of power / ITPC. In our study, children with ASD had reduced ITPC in the right auditory cortex, Wilson et al. (2007) reported a left-hemispheric decrease of ASSR, whereas Seymour et al. (2020) found a bilateral reduction of this neural response. Perhaps, both children's age and stimulus presentation (monaural vs. binaural) contributed to these differences.

In general, the gamma-band abnormalities in autism were reported in numerous studies (Contractor et al., 2021; Gabard-Durnam et al., 2019; Rojas et al., 2008; Rojas and Wilson, 2014; Snijders et al., 2013; Zikopoulos and Barbas, 2013) and are considered by some authors as the potential neural marker of this disorder (e.g., Gandal et al., 2010; Rojas and Wilson, 2014). Gamma oscillations are intimately related to E / I balance and they arise from the inhibition of pyramidal cells by fast-spiking PV+ interneurons via binding of the inhibitory neurotransmitter GABA (Agetsuma et al., 2018; Cardin et al., 2009; Carlén et al., 2012). Therefore, the reduction of 40 Hz ASSR in children with ASD may reflect a dysregulated neural inhibition, resulting in imbalance between E and I (Rubenstein and Merzenich, 2003; Sohal and Rubenstein, 2019). Importantly, some studies with the same age-range group of participants did not find the differences in 40 Hz ASSR between children with and without ASD (Edgar et al., 2016; Ono et al., 2020; Stroganova et al., 2020). Despite methodological differences across the studies as well as

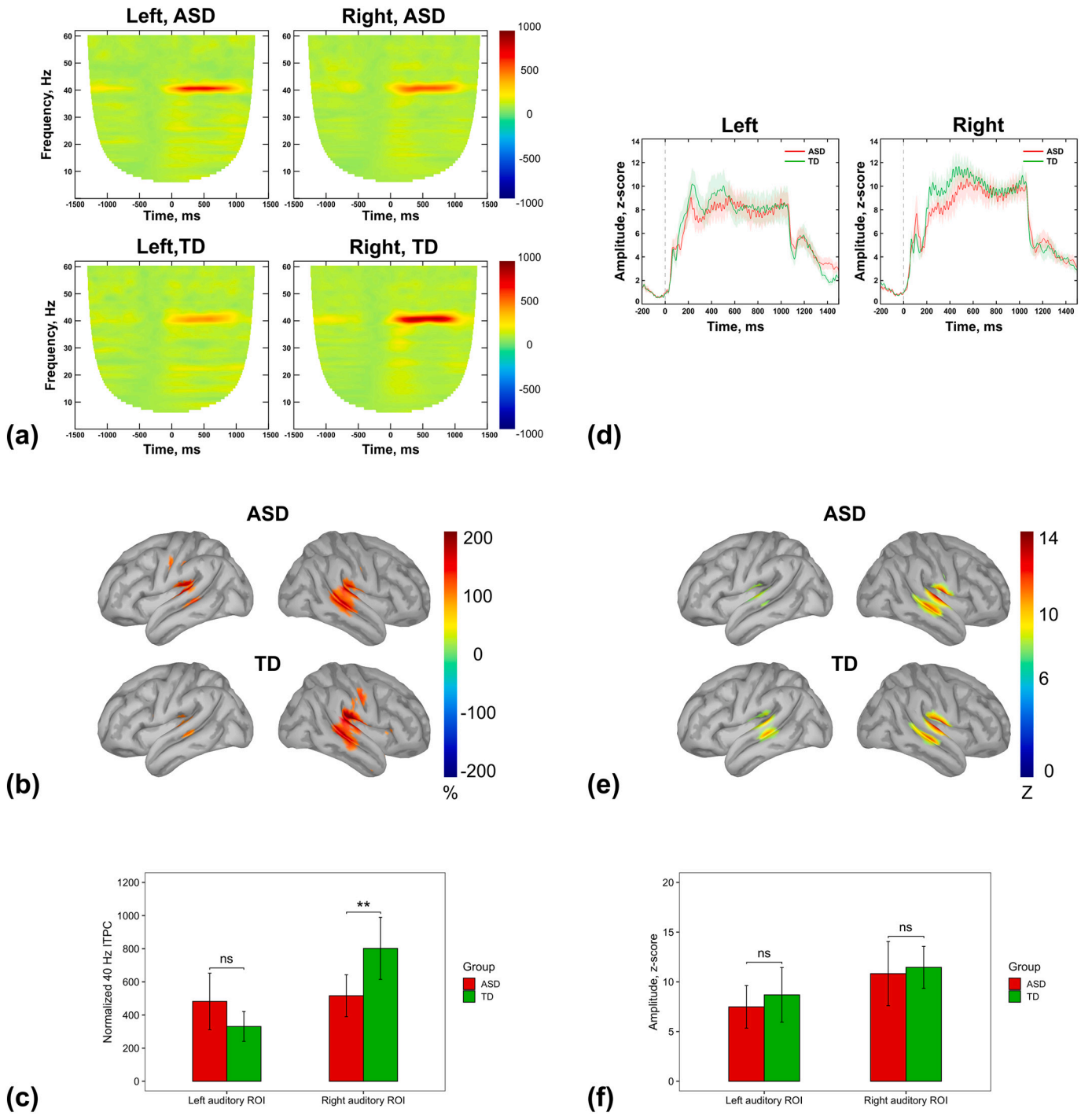

Fig. 4. The comparison of Auditory Steady-State Response (ASSR) and sustained Event-Related Field (ERF) between ASD and TD groups of children: (a) Time-frequency maps for the left and right auditory ROIs (normalized ITPC-values, % change from the baseline); (b) Distribution of 40 Hz ASSR across the cortex in the left and right hemispheres averaged in a 200–900 ms time interval (the amplitude threshold is set at 70% of the highest values); (c) Group differences in 40 Hz ASSR in left and right ROIs; (d) Timecourses of the ERF response in the left and right ROIs; (e) Distribution of *z*-score absolute values in the left and right hemispheres averaged in a 200–1000 ms time interval (sustained parts of ERF, the amplitude threshold is set at 70% of the highest values); (f) Group differences in ERF amplitude in left and right ROIs.

relatively small sample sizes, a highly heterogeneous nature of the ASD population may contribute to inconsistencies in these findings. For example, some authors (Neklyudova et al., 2021; Sivarao et al., 2016) propose that 40 Hz ASSR is related to the *N*-methyl-D-aspartate (NMDA) receptors on PV+ cells and, thus, reduced 40 Hz ASSR may be associated not with the whole ASD population, but rather with a specific genetic subgroup of individuals with ASD who have a dysfunction of NMDA receptors. Dickinson et al. (2016) have also mentioned that different subgroups of ASD can have different neural profiles with respect to E / I balance.

Contrary to the atypical decrease of 40 Hz steady-state auditory gamma response in children with ASD from our sample, we did not find significant between-group differences in sustained ERF in any hemisphere. To the best of our knowledge, there is only one MEG study

Table 4
The comparison of the sustained part of Event-Related Fields (ERFs) between ASD and TD groups of children.

	Sustained part of ERF			
Predictors	Estimate	Standard error	*t*	*p*
(Intercept)	9.16	0.88	10.43	**<0.001*****
Hemisphere_Left	−1.67	0.88	−1.90	0.061
Hemisphere_Left:TD_group	1.21	1.76	0.69	0.494
Hemisphere_Right: TD_group	0.63	1.76	0.36	0.721
Observations	80			
R^2 / R^2 adjusted	0.080 / 0.044			

focused on sustained ERF in children with ASD (Stroganova et al., 2020). This study provides the evidence of the left-hemispheric deficit in sustained ERF discussing the possible relationship between this response and pitch processing in children with ASD. Note, however, that in this study, the sources of ASSR and ERF were different, and the authors did not aim to measure the evoked response of the same cortical region as for ASSR. Therefore, we cannot directly compare our findings with the previous ones.

4.3. The laterality of 40 Hz ASSR and the age-related changes of ASSR and ERF responses in children with and without ASD

First, in both groups of children, we showed a right-hemispheric dominance of ASSR, indicating that 40 Hz ITPC was significantly higher in the right auditory cortex. This means that the pattern and asymmetry of 40 Hz ASSR in children with ASD were the same as in TD children, although the ASD group had a reduced 40 Hz ITPC in the right hemisphere. Note that the presence of 40 Hz ASSR dominantly in the right hemisphere has been observed in the previous studies localizing this response in children with and without ASD (Edgar et al., 2016; Ono et al., 2020; Poulsen et al., 2009; Stroganova et al., 2020) and also in adults (e.g., Pellegrino et al., 2019; Ross et al., 2005). This asymmetry of ASSR was explained with a right-hemispheric specialization of processing the temporal periodicity of a sound (Ross et al., 2005) and earlier development of the right auditory cortex in comparison to the left (Edgar et al., 2016; Poulsen et al., 2009). Overall, the hemispheric asymmetry of auditory response can be related to morphological and functional differences between left and right auditory cortices (Boemio et al., 2005; Devlin et al., 2003; Hine and Debener, 2007). Regardless of the explanation, our findings showed that children with ASD had a typical hemispheric specialization of 40 Hz ASSR.

Second, the age-related changes in 40 Hz ASSR, which were observed in TD children, were not presented in children with ASD. In our TD group, as well as in the previous studies focusing on the developmental changes of ASSR, the age-related increase in the strength of 40 Hz ASSR has been demonstrated (Arutiunian et al., 2022a; Cho et al., 2015; Edgar et al., 2016; Seymour et al., 2020; Stroganova et al., 2020). Moreover, some authors mentioned that it is very difficult to detect this response in very young children and highlighted that 40 Hz ASSR became more stable with age (Maurizi et al., 1990; Stapells et al., 1988). It was hypothesized that the increase of 40 Hz ITPC with age could be related to the maturation of GABAergic inhibitory neurotransmission and developmental changes of E / I balance (Cho et al., 2015). In general, this development starts early in the neonate brain by switching from a depolarizing to hyperpolarizing action of GABA receptors (Ben-Ari,

Table 5
The associations between 40 Hz Auditory Steady-State Response and the amplitude of the sustained part of Event-Related Fields in the left and right auditory ROIs in children with ASD.

	40 Hz Inter-Trial Phase Consistency							
	ASD				TD			
Predictors	*Estimate*	*Standard error*	*t*	*p*	*Estimate*	*Standard error*	*t*	*p*
(Intercept)	294.46	82.49	3.57	**0.001****	837.24	87.56	9.56	**<0.001*****
Hemisphere_Left	−217.61	76.77	−2.83	**0.008****	−576.78	81.93	−7.04	**<0.001*****
Hemisphere_Left:Amplitude	54.11	13.06	4.14	**<0.001*****	8.09	8.64	0.94	0.34
Hemisphere_Right:Amplitude	0.38	8.65	0.04	0.96	−53.41	11.24	−4.75	**<0.001*****
Random Effects								
σ^2	56,161.99				32,387.06			
$\tau_{00\ ID}$	14,459.32				32,946.70			
ICC	0.20				0.50			
N_{ID}	20				20			
Observations	40				40			
Marginal R^2 / Conditional R^2	0.299 / 0.442				0.569 / 0.787			

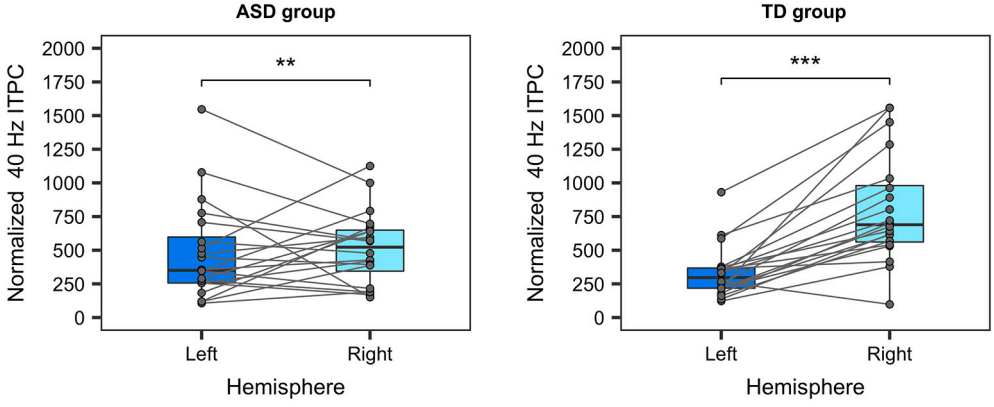

Fig. 5. The hemispheric differences in 40 Hz Auditory Steady-State Response in children with and without ASD.

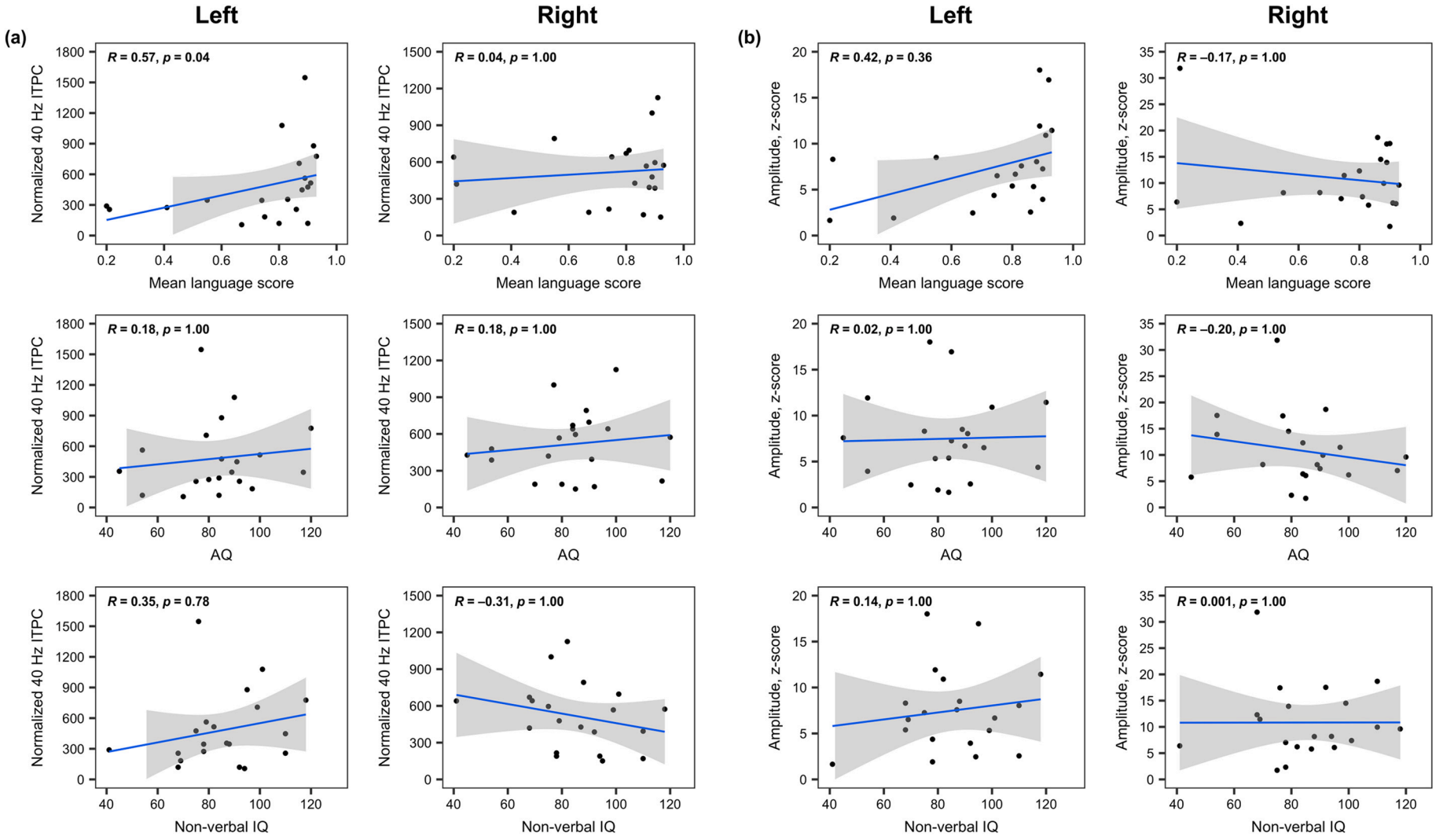

Fig. 6. The relationships between neural responses and individual characteristics in children with ASD (all *p*-values are Bonferroni-corrected): (a) 40 Hz ITPC as a function of mean language score, severity of autistic symptoms (AQ), and non-verbal IQ; (b) ERF amplitude as a function of mean language score, severity of autistic symptoms (AQ), and non-verbal IQ.

2002, 2014; Cherubini et al., 1991). In the group of children with ASD, we did not find this age-associated pattern, which addressed the atypical developmental state of 40 Hz ASSR in these children.

The relationships between the amplitude of sustained ERF and age were similar in both groups of children, indicating that this type of neural response did not change with age. Note, however, that in TD group, there was a marginally significant effect after correction for multiple comparisons and also there was a significant age-related decrease of the amplitude of sustained ERF in a larger group of TD children (see Arutiunian et al., 2022a). Some previous MEG / EEG studies have also demonstrated an age-related decrease in strength of the transient auditory components (P1, N1, and N2) in children (e.g., Ceponiene et al., 2002; Ponton et al., 2000; Poulsen et al., 2009; Takeshita et al., 2002). One of the potential explanations of this developmental pattern in both transient and sustained evoked potentials can be the drop of synaptic density after 10 years of age and an advance of intra-cortical myelination (see Ponton et al., 2000; Poulsen et al., 2009).

Finally, in TD children, there was a negative relationship between 40 Hz TTPC and the amplitude of sustained ERF, so that the higher ITPC was associated with the lower source amplitude in the right auditory cortex. We did not observe this effect in children with ASD. Moreover, we found an atypical significant relationship between 40 Hz ITPC and the amplitude of sustained ERF in the left auditory cortex, indicating that the higher 40 Hz ITPC was related to the higher source amplitude.

To sum up, all these differences between children with and without ASD regarding the age-related changes and relationships between both types of auditory responses (40 Hz ASSR and sustained ERF) reflect, broadly, atypical developmental state of the auditory cortex in children with ASD which is consisted with the previous studies (e.g., Roberts et al., 2010, 2019, 2021).

4.4. The relationships between auditory responses and behavioral measures in children with ASD

In order to reveal whether the auditory responses (40 Hz ASSR and sustained ERF) are related to behavioral measures (non-verbal IQ, the severity of autistic symptoms, and language abilities) in children with ASD, we run Pearson's correlations. The results demonstrated no significant associations between the amplitude of sustained ERF in any hemisphere and non-verbal IQ, the severity of autism, or the language abilities of children with ASD.

The analysis of the relationship between 40 Hz ITPC and non-verbal IQ in children with autism did not reveal a significant correlation. Our results are consistent with the previous findings, indicating that the strength of 40 Hz ASSR is not associated with non-verbal cognition of children and adolescents with ASD (Seymour et al., 2020; Stroganova et al., 2020; Wilson et al., 2007). We also did not find a relationship between the severity of autistic symptoms (measured with the AQ questionnaire) and 40 Hz ASSR. These results corresponded to those reported by Seymour et al. (2020) and opposite to those presented in Stroganova et al. (2020). This discrepancy may be related not only to the heterogeneity in ASD population but also to the assessment tool, i.e., AQ is not a direct measure of child behavior but parental report.

Importantly, we demonstrated a significant association between 40 Hz steady-state gamma response in the language-dominant left auditory cortex and the language abilities of children with ASD. Particularly, our findings indicated that the lower 40 Hz ITPC in the left hemisphere was related to more impaired language comprehension in children with ASD. This means that sensory gamma oscillations and the ability of low-level neural synchronization at the gamma frequency in the primary auditory cortex are essential for language comprehension in children with ASD. Although we did not find a between-group difference in 40 Hz ITPC in the left hemisphere, our findings highlighted the crucial role of the low-level sensory perception in language processing in children with ASD. This is in line with Roberts et al. (2021) study with amplitude-modulated sweeps indicated that ITPC at a gamma-band is associated with language skills in children with ASD. The authors concluded that the electrophysiological signature associated with E / I imbalance has, therefore, a clinical / behavioral consequence. Several previous studies have shown that the gamma-band oscillations in the left auditory cortex are specifically needed for coding temporal fine units of speech (Giraud et al., 2007; Giraud and Poeppel, 2012; Moon et al., 2022; Poeppel and Assaneo, 2020), analyzing the properties of a sound in a short temporal integration windows (Hämäläinen et al., 2012; Poeppel, 2003). Therefore, all these processes in the left primary auditory cortex can be intimately related to language functioning in autism. Remarkably, according to different studies, the resting-state or baseline gamma oscillations are also associated with the language abilities of both children with idiopathic ASD and children with single-gene disorders related to ASD (i.e., Fragile X syndrome), and can even be an early biomarker of further language functioning in ASD (Romeo et al., 2021; Wilkinson et al., 2019; Wilkinson and Nelson, 2021).

Summarizing, our findings showed that 40 Hz ASSR in children with ASD was related only to language abilities but not to other cognitive domains (non-verbal IQ and social functioning measured with AQ). The relation was observed only for 40 Hz ASSR in the language-dominant left hemisphere.

5. Limitations and future directions

We acknowledge some limitations of our study. First, the sample of children is small which can result in low statistical power. In order to generalize the observed effects (especially within-group relationships between brain and behavior), it is necessary to include a larger sample size. Second, we used amplitude-modulated tones only with the duration at 1000 ms. At the same time, inconsistencies across different studies may be partly related to different duration of auditory stimulation (e.g., 500 ms in Stroganova et al. (2020) and 1500 ms in Seymour et al. (2020)). Thus, it would be beneficial to use stimuli varying in their duration in the same groups of children with and without ASD. This will help to clarify whether the duration of stimuli influences gamma synchronization in the auditory cortex in children with ASD. Third, the study did not provide any behavioral measures of sensory sensitivity to assess auditory hyper/hypo-reactivity and to analyze the relationships between these measures and auditory cortical responses. Fourth, we did not account for individual differences in hearing thresholds and loudness perception which can play a role in the strengths of both types of auditory responses. Finally, our study examined the age-related changes of 40 Hz ASSR and the sustained ERF cross-sectionally. Future studies would benefit from using a longitudinal design to analyze the functional maturational changes in the primary auditory cortex in children with and without ASD.

6. Conclusions

In the present study, we found that primary-school-aged children with ASD had a reduced 40 Hz steady-state auditory gamma response and the age-related abnormalities in both types of responses (ASSR and ERF). These atypicalities may reflect a dysregulated neural inhibition, leading to the imbalance between E and I in the primary auditory cortex. Moreover, our study provided the first evidence of the relationship between 40 Hz ASSR in the language-dominant left auditory cortex and language comprehension in children with ASD. Although the study included a small sample size with a large age-range of participants, the results highlighted the significant low-level neural mechanisms in the auditory cortex that are related to the language abilities of children with ASD. Perhaps, if future research with the same paradigm but larger sample size will confirm our results, 40 Hz ASSR could be used as one of the potential biomarkers of language development in children with ASD.

Funding

The study was supported by the Russian Science Foundation, Project No 22-28-01261 (collection and analysis of the data of 20 typically developing children and 10 children with ASD). The contribution of Irina Buyanova and Olga Dragoy (collection and analysis of the data of 10 children with ASD) was supported by the Basic Research Program at the National Research University Higher School of Economics.

Disclosure statement

The authors have no conflict of interest to disclose.

Ethical statement

The study was approved by the ethics committee of Moscow State University of Psychology and Education (for ASD group) and the HSE University Committee on Interuniversity Surveys and Ethical Assessment of Empirical Research (for TD group), and was conducted following the ethical principles regarding human experimentation (the Declaration of Helsinki). All children and their parents provided the verbal assent to participate in the study and were informed that they can withdraw from the study at any time during the experiment. A written consent form was obtained from a parent of each child.

CRediT authorship contribution statement

Vardan Arutiunian: Conceptualization, Methodology, Investigation, Data curation, Formal analysis, Writing – original draft, Writing – review & editing, Project administration. **Giorgio Arcara:** Methodology, Formal analysis, Writing – review & editing. **Irina Buyanova:** Investigation. **Elizaveta Davydova:** Investigation. **Darya Pereverzeva:** Investigation. **Alexander Sorokin:** Investigation. **Svetlana Tyushkevich:** Investigation. **Uliana Mamokhina:** Investigation. **Kamilla Danilina:** Investigation. **Olga Dragoy:** Writing – review & editing, Resources.

Acknowledgments

We thank Roman Cheremin for providing access to the resources of the Center for Speech Pathology and Neurorehabilitation, Moscow, Russia. We also thank Olga Buivolova and Natalia Deeva for their assistance with participant recruitment in the MRI part of the study. The study was implemented at the unique research facility "Center for Neurocognitive Research (MEG-Center)" in MSUPE. Special thanks go to all children who enthusiastically participated in the study.

Appendix A. Supplementary data

Supplementary data to this article can be found online at https://doi.org/10.1016/j.pnpbp.2022.110690.

References

Agetsuma, M., Hamm, J.P., Tao, K., Fujisawa, S., Yuste, R., 2018. Parvalbumin-positive interneurons regulate neuronal ensembles in visual cortex. Cereb. Cortex 28, 1831–1845. https://doi.org/10.1093/cercor/bhx169.

American Psychiatric Association, 2013. Diagnostic and Statistical Manual of Mental Disorders: DSM-5, 5th ed. American Psychiatric Publication, Washington, DC; London, p. 947.

Arutiunian, V., Arcara, G., Buyanova, I., Gomozova, M., Dragoy, O., 2022a. The age-related changes in 40 Hz auditory steady-state response and sustained event-related fields to the same amplitude-modulated tones in typically developing children: a magnetoencephalography (MEG) study. Hum. Brain Mapp. 43 (1–14), 5370–5383. https://doi.org/10.1002/hbm.26013.

Arutiunian, V., Lopukhina, A., Minnigulova, A., Shlyakhova, A., Davydova, E., Pereverzeva, D., Sorokin, A., Tyushkevich, S., Mamokhina, U., Danilina, K., Dragoy, O., 2022b. Language abilities of Russian primary-school-aged children with autism Spectrum disorder: evidence from comprehensive assessment. J. Autism Dev. Disord. 52, 584–599. https://doi.org/10.1007/s10803-021-04967-0.

Atallah, B.V., Scanziani, M., 2009. Instantaneous modulation of gamma oscillations frequency by balancing excitation with inhibition. Neuron 62, 566–577. https://doi.org/10.1016/j.neuron.2009.04.027.

Auyeung, B., Baron-Cohen, S., Wheelwright, S., Allison, C., 2008. The autism spectrum quotient: Children's version (AQ-child). J. Autism Dev. Disord. 38, 1230–1240. https://doi.org/10.1007/s10803-007-0504-z.

Bartos, M., Vida, I., Jonas, P., 2007. Synaptic mechanisms of synchronized gamma oscillations in inhibitory interneuron networks. Nat. Rev. Neurosci. 8, 45–56. https://doi.org/10.1038/nrn2044.

Bates, D., Mächler, M., Bolker, B.M., Walker, S.C., 2015. Fitting linear mixed-effects models using lme4. J. Stat. Softw. 67, 1–48. https://doi.org/10.18637/jss.v067.i01.

Ben-Ari, Y., 2002. Excitatory actions of GABA during development: the nature of the nurture. Nat. Rev. Neurosci. 3, 728–739. https://doi.org/10.1038/nrn920.

Ben-Ari, I., 2014. The GABA excitatory / inhibitory developmental sequence: a personal journey. Neuroscience 279, 187–219. https://doi.org/10.1016/j.neuroscience.2014.08.001.

Berman, J.I., Edgar, J.C., Blaskey, L., Kuschner, E.S., Levy, S.E., Ku, M., Dell, J., Roberts, T.P.L., 2016. Multimodal diffusion-MRI and MEG assessment of auditory and language system development in autism spectrum disorder. Front. Neurosci. 10, 30. https://doi.org/10.3389/fnana.2016.00030.

Boemio, A., Fromm, S., Braun, A., Poeppel, D., 2005. Hierarchical and asymmetric temporal sensitivity in human auditory cortices. Nat. Neurosci. 8, 389–395. https://doi.org/10.1038/nn1409.

Brown, C., Gruber, T., Boucher, J., Rippon, G., Brock, J., 2005. Gamma abnormalities during perception of illusory figures in autism. Cortex 41, 364–376. https://doi.org/10.1016/s0010-9452(08)70273-9.

Cardin, J.A., Carlén, M., Meletis, K., Knoblich, U., Zhang, F., Deisseroth, K., Tsai, L.-H., Moore, C.I., 2009. Driving fast-spiking cells induces gamma rhythm and controls sensory responses. Nature 459, 663–668. https://doi.org/10.1038/nature08002.

Carlén, M., Meletis, K., Siegle, J.H., Cardin, J.A., Futai, K., Vierling-Claassen, D., Rühlmann, C., Jones, S.R., Deisseroth, K., Sheng, M., Moore, C.I., Tsai, L.-H., 2012. A critical role for the NMDA receptors in parvalbumin interneurons for gamma rhythm induction and behavior. Mol. Psychiatry 17, 537–548. https://doi.org/10.1038/mp.2011.31.

Ceponiene, R., Rinne, T., Näätänen, R., 2002. Maturation of cortical sound processing as indexed by event-related potentials. Clin. Neurophysiol. 113, 870–882. https://doi.org/10.1016/s1388-2457(02)00078-0.

Cherubini, E., Gaiarsa, J.L., Ben-Ari, Y., 1991. GABA: an excitatory transmitter in early postnatal life. Trends Neurosci. 14, 515–519. https://doi.org/10.1016/0166-2236(91)90003-D.

Cho, R.Y., Walker, C.P., Polizzotto, N.R., Wozny, T.A., Fissell, C., Chen, C.-M.A., Lewis, D.A., 2015. Development of sensory gamma oscillations and cross-frequency coupling from childhood to early adulthood. Cereb. Cortex 25, 1509–1518. https://doi.org/10.1093/cercor/bht341.

Contractor, A., Ethell, I.M., Portera-Cailliau, C., 2021. Cortical interneurons in autism. Nat. Neurosci. 24, 1648–1659. https://doi.org/10.1038/s41593-021-00967-6.

Dale, A.M., Fischl, B., Sereno, M.I., 1999. Cortical surface-based analysis: I. Segmentation and surface reconstruction. NeuroImage 9, 179–194. https://doi.org/10.1006/nimg.1998.0395.

Delorme, A., Makeig, S., 2004. EEGLAB: an open source toolbox for analysis of single-trial EEG dynamics including independent component analysis. J. Neurosci. Methods 134, 9–21. https://doi.org/10.1016/j.jneumeth.2003.10.009.

Destrieux, C., Fischl, B., Dale, A., Halgren, E., 2010. Automatic parcellation of human cortical gyri and sulci using standard anatomical nomenclature. NeuroImage 53, 1–15. https://doi.org/10.1016/j.neuroimage.2010.06.010.

Devlin, J.T., Raley, J., Tunbridge, E., Lanary, K., Floyer-Lea, A., Narain, C., Cohen, I., Behrens, T., Jezzard, P., Matthews, P.M., Moore, D.R., 2003. Functional asymmetry for auditory processing in human primary auditory cortex. J. Neurosci. 23, 11516–11522. https://doi.org/10.1523/JNEUROSCI.23-37-11516.2003.

Dickinson, A., Jones, M., Milne, E., 2016. Measuring neural excitation and inhibition in autism: different approaches, different findings and different interpretations. Brain Res. 1648 (A), 277–289. https://doi.org/10.1016/j.brainres.2016.07.011.

Diedenhofen, B., Musch, J., 2015. Cocor: a comprehensive solution for the statistical comparison of correlations. PLoS One 10, e0121945. https://doi.org/10.1371/journal.pone.0121945.

Dwyer, P., Wang, X., Meo-Monteil, R., Hsieh, F., Saron, C.D., Rivera, S.M., 2020. Defining clusters of young autistic and typically developing children based on loudness-dependent auditory electrophysiological responses. Mol. Autism 11, 48. https://doi.org/10.1186/s13229-020-00352-3.

Edgar, J.C., Fisk 4th, C.L., Liu, S., Pandey, J., Herrington, J.D., Schultz, R.T., Roberts, T.P.L., 2016. Translating adult electrophysiology findings to younger patient populations: difficulty measuring 40-Hz auditory steady-state response in typically developing children and children with autism spectrum disorder. Dev. Neurosci. 38, 1–14. https://doi.org/10.1159/000441943.

Espinoza, C., Guzman, S.J., Zhang, X., Jonas, P., 2018. Parvalbumin+ interneurons obey unique connectivity rules and establish a powerful lateral-inhibition microcircuit in dentate gyrus. Nat. Commun. 9, 4605. https://doi.org/10.1038/s41467-018-06899-3.

Farahani, E.D., Wouters, J., Wieringen, A., 2021. Brain mapping of auditory steady-state responses: a broad view of cortical and subcortical sources. Hum. Brain Mapp. 42, 780–796. https://doi.org/10.1002/hbm.25262.

Ferguson, B.R., Gao, W.-J., 2018. PV interneurons: critical regulators of E / I balance for prefrontal cortex-dependent behavior and psychiatric disorders. Front. Neural Circ. 12, 37. https://doi.org/10.3389/fncir.2018.00037.

Ford, T.C., Abu-Akel, A., Crewther, D.P., 2019. The association of excitation and inhibition signaling with the relative symptom expression of autism and psychosis-proneness: implications for psychopharmacology. Prog. Neuro-Psychopharmacol. Biol. Psychiatry 88, 235–242. https://doi.org/10.1016/j.pnpbp.2019.109769.

Ford, T.C., Woods, W., Enticott, P.G., Crewther, D.P., 2020. Cortical excitation-inhibition ratio mediates the effect of pre-attentive auditory processing deficits on interpersonal difficulties. Prog. Neuro-Psychopharmacol. Biol. Psychiatry 98, 109769. https://doi.org/10.1016/j.pnpbp.2019.109769.

Gabard-Durnam, L.J., Wilkinson, C., Kapur, K., Tager-Flusberg, H., Levin, A.R., Nelson, C.A., 2019. Longitudinal EEG power in the first postnatal year differentiates autism outcome. Nat. Commun. 10, 4188. https://doi.org/10.1038/s41467-019-12202-9.

Gandal, M.J., Edgar, J.C., Ehrlichman, R.S., Mehta, M., Roberts, T.P.L., Siegel, S.J., 2010. Validating γ oscillations and delayed auditory responses as translational biomarkers of autism. Biol. Psychiatry 68, 1100–1106. https://doi.org/10.1016/j.biopsych.2010.09.031.

Giraud, A.-L., Poeppel, D., 2012. Cortical oscillations and speech processing: emerging computational principles and operations. Nat. Neurosci. 15, 511–517. https://doi.org/10.1038/nn.3063.

Giraud, A.-L., Kleinschmidt, A., Poeppel, D., Lund, T.E., Frackwiak, R.S.J., Laufs, H., 2007. Endogenous cortical rhythms determine cerebral specialization for speech perception and production. Neuron 56, 1127–1134. https://doi.org/10.1016/j.neuron.2007.09.038.

Hämäläinen, M.S., Ilmoniemi, R.J., 1994. Interpreting magnetic fields of the brain: minimum norm estimates. Med. Biol. Eng. Comput. 32, 35–42. https://doi.org/10.1007/BF02512476.

Hämäläinen, J.A., Rupp, A., Soltész, F., Szücs, D., Goswami, U., 2012. Reduced phase locking to slow amplitude modulation in adults with dyslexia: an MEG study. NeuroImage 59, 2952–2961. https://doi.org/10.1016/j.neuroimage.2011.09.075.

Harrell Jr., F.E., Dupont, C., 2020. Hmisc: Harrell Miscellaneous. R package version 4.4.0. URL. https://CRAN.R-project.org/package=Hmisc.

Hine, J., Debener, S., 2007. Late auditory evoked potentials asymmetry revisited. Clin. Neurophysiol. 118, 1274–1285. https://doi.org/10.1016/j.clinph.2007.03.012.

Huang, M.X., Mosher, J.C., Leahy, R.M., 1999. A sensor-weighted overlapping-sphere head model and exhaustive head model comparison for MEG. Phys. Med. Biol. 44, 423–440. https://doi.org/10.1088/0031-9155/44/2/010.

Kaufman, A.S., Kaufman, N.L., 2004. Kaufman Assessment Battery for Children, 2nd ed. American Guidance Service.

Keceli, S., Okamoto, H., Kakigi, R., 2015. Hierarchical neural encoding of temporal regularity in the human auditory cortex. Brain Topogr. 28, 459–470. https://doi.org/10.1007/s10548-013-0300-3.

Kessler, K., Seymour, R.A., Rippon, G., 2016. Brain oscillations and connectivity in autism spectrum disorders (ASD): new approaches to methodology, measurement and modelling. Neurosci. Biobehav. Rev. 71, 601–620. https://doi.org/10.1016/j.neubiorev.2016.10.002.

Kjelgaard, M.M., Tager-Flusberg, H., 2001. An investigation of language impairment in autism: implications for genetic subgroups. Lang. Cogn. Process. 16, 287–308. https://doi.org/10.1080/01690960042000058.

Korczak, P., Smart, J., Delgado, R., Strobel, T.M., Bradford, C., 2012. Auditory steady-state responses. J. Am. Acad. Audiol. 23, 146–170. https://doi.org/10.3766/jaaa.23.3.3.

Levin, A.R., Nelson, C.A., 2015. Inhibition-based biomarkers for autism spectrum disorder. Neurotherapeutics 12, 546–552. https://doi.org/10.1007/s13311-015-0350-1.

Lin, Fa-H, Witzel, T., Ahlfors, S.P., Stufflebeam, S.M., Belliveau, W., Hämäläinen, M.S., 2006. Assessing and improving the spatial accuracy in MEG source localization by depth-weighted minimum-norm estimates. NeuroImage 31, 160–171. https://doi.org/10.1016/j.neuroimage.2005.11.054.

Lord, C., Rutter, M., DiLavore, P.C., Risi, S., Gotham, K., Bishop, S.L., 2012. Autism Diagnostic Observation Schedule, 2nd ed. Western Psychological Services.

Lüdecke, D., 2020. sjPlot: Data Visualization for Statistics in Social Science. R package version 2.8.4. URL. https://CRAN.R-project.org/package=sjPlot.

Magueresse, C.L., Monyer, H., 2013. GABAergic interneurons shape the functional maturation of the cortex. Neuron 77, 388–405. https://doi.org/10.1016/j.neuron.2013.01.011.

Matsuzaki, J., Kagitani-Shimono, K., Sugata, H., Hirata, M., Hanaie, R., Nagatani, F., Tachibana, M., Tominaga, K., Mohri, I., Taniike, M., 2014. Progressively increased M50 responses to repeated sounds in autism Spectrum disorder with auditory hypersensitivity: a magnetoencephalographic study. PLoS One 9, e102599. https://doi.org/10.1371/journal.pone.0102599.

Matsuzaki, J., Kuschner, E.S., Blaskey, L., Bloy, L., Kim, M., Ku, M., Edgar, J.C., Embick, D., Roberts, T.P.L., 2019. Abnormal auditory mismatch fields are associated with communication impairment in both verbal and minimally verbal / nonverbal children who have autism spectrum disorder. Autism Res. 12, 1225–1235. https://doi.org/10.1002/aur.2136.

Maurizi, M., Almadori, G., Paludetti, G., Ottaviani, F., Rosignoli, M., Luciano, R., 1990. 40-Hz steady-state responses in newborns and in children. Audiology 29, 322–328. https://doi.org/10.3109/00206099009072863.

McFadden, K.L., Steinmetz, S.E., Carroll, A.M., Simon, S.T., Wallace, A., Rojas, D.C., 2014. Test-retest reliability of the 40 Hz EEG auditory steady-state response. PLoS One 9, e85748. https://doi.org/10.1371/journal.pone.0085748.

Moon, J., Orlandi, S., Chau, T., 2022. A comparison and classification of oscillatory characteristics in speech perception and covert speech. Brain Res. 1781, 147778 https://doi.org/10.1016/j.brainres.2022.147778.

Nash-Kille, A., Sharma, A., 2014. Inter-trial coherence as a marker of cortical phase synchrony in children with sensorineural hearing loss and auditory neuropathy spectrum disorder fitted hearing aids and cochlear implants. Clin. Neurophysiol. 125, 1459–1470. https://doi.org/10.1016/j.clinph.2013.11.017.

Neklyudova, A., Portnova, G.V., Rebreikina, A.B., Voinova, V.Y., Vorsanova, S.G., Iourov, I.Y., Sysoeva, O.V., 2021. 40-Hz auditory steady-state response (ASSR) as a biomarker of genetic defects in the *SHANK3* gene: a case report of 15-year-old girl with a rare partial *SHANK3* duplication. Int. J. Mol. Sci. 22, 1898. https://doi.org/10.3390/ijms22041898.

Ono, Y., Kudoh, K., Ikeda, T., Takahashi, T., Yoshimura, Y., Minabe, Y., Kikuchi, M., 2020. Auditory steady-state response at 20 Hz and 40 Hz in young typically developing children and children with autism spectrum disorder. Psychiatry Clin. Neurosci. 74, 354–360. https://doi.org/10.1111/pcn.12998.

Peirce, J.W., 2007. PsychoPy – psychophysics software in Python. J. Neurosci. Methods 162, 8–13. https://doi.org/10.1016/j.jneumeth.2006.11.017.

Pellegrino, G., Arcara, G., Di Pino, G., Turco, C., Maran, M., Weis, L., Piccione, F., Siebner, H.R., 2019. Transcranial direct current stimulation over the sensory-motor regions inhibit gamma synchrony. Hum. Brain Mapp. 40, 2736–2746. https://doi.org/10.1002/hbm.24556.

Pickles, A., Anderson, D.K., Lord, C., 2014. Heterogeneity and plasticity in the development of language: a 17-year follow-up of children referred early for possible autism. J. Child Psychol. Psychiatry 55, 1354–1362. https://doi.org/10.1111/jcpp.12269.

Poeppel, D., 2003. The analysis of speech in different temporal integration windows: cerebral lateralization as 'asymmetric sampling in time'. Speech Comm. 41, 245–255. https://doi.org/10.1016/S0167-6393(02)00107-3.

Poeppel, D., Assaneo, M.F., 2020. Speech rhythms and their neural foundations. Nat. Rev. Neurosci. 21, 322–334. https://doi.org/10.1038/s41583-020-0304-4.

Ponton, C., Eggermont, J.J., Kwong, B., Don, M., 2000. Maturation of human central auditory system activity: evidence from multi-channel evoked potentials. Clin. Neurophysiol. 111, 220–236. https://doi.org/10.1016/s1388-2457(99)00236-9.

Poulsen, C., Picton, T., Paus, T., 2009. Age-related changes in transient and oscillatory brain responses to auditory stimulation during early adolescence. Dev. Sci. 12, 220–235. https://doi.org/10.1111/j.1467-7687.2008.00760.x.

R Core Team, 2019. R: A Language and Environment for Statistical Computing. R Foundation for Statistical Computing, Vienna. URL. https://www.R-project.org/.

Raven, J., 2000. The Raven's progressive matrices: change and stability over culture and time. Cogn. Psychol. 41, 1–48. https://doi.org/10.1006/cogp.1999.0735.

Roach, B.J., D'Souza, D.C., Ford, J.M., Mathalon, D.H., 2019. Test-retest reliability of time-frequency measures of auditory steady-state responses in patients with schizophrenia and healthy controls. NeuroImage 23, 101878. https://doi.org/10.1016/j.nicl.2019.101878.

Roberts, T.P.L., Khan, S.Y., Rey, M., Monroe, J.F., Cannon, K., Blaskey, L., Woldoff, S., Qasmieh, S., Gandal, M., Schmidt, G.L., Zarnow, D.M., Levy, S.E., Edgar, J.C., 2010. MEG detection of delayed auditory evoked responses in autism spectrum disorders: towards an imaging biomarker for autism. Autism Res. 3, 8–18. https://doi.org/10.1002/aur.111.

Roberts, T.P.L., Cannon, K.M., Tavabi, K., Blaskey, L., Khan, S.Y., Monroe, J.F., Qasmieh, S., Levy, S.E., Edgar, J.C., 2011. Auditory magnetic mismatch field latency: a biomarker for language impairment in autism. Biol. Psychiatry 70, 263–269. https://doi.org/10.1016/j.biopsych.2011.01.015.

Roberts, T.P.L., Matsuzaki, J., Blaskey, L., Bloy, L., Edgar, C.J., Kim, M., Ku, M., Kuschner, E.S., Embick, D., 2019. Delayed M50/M100 evoked response component latency in minimally verbal / nonverbal children who have autism spectrum disorder. Mol. Autism 10, 34. https://doi.org/10.1186/s13229-019-0283-3.

Roberts, T.P.L., Bloy, L., Liu, S., Ku, M., Blaskey, L., Jackel, C., 2021. Magnetoencephalography studies of the envelope following response during amplitude-modulated sweeps: diminished phase synchrony in autism Spectrum disorder. Front. Hum. Neurosci. 15, 787229 https://doi.org/10.3389/fnhum.2021.787229.

Robertson, C.E., Baron-Cohen, S., 2017. Sensory perception in autism. Nat. Rev. Neurosci. 18, 671–684. https://doi.org/10.1038/nrn.2017.112.

Rojas, D.C., Wilson, L.B., 2014. γ-Band abnormalities as markers of autism spectrum disorders. Biomark. Med 8, 353–368. https://doi.org/10.2217/bmm.14.15.

Rojas, D.C., Maharajh, K., Teale, P., Rogers, S.J., 2008. Reduced neural synchronization of gamma-band MEG oscillations in first-degree relatives of children with autism. BMC Psychiatry 8, 66. https://doi.org/10.1186/1471-244X-8-66.

Rojas, D.C., Teale, P.D., Maharajh, K., Kronberg, E., Youngpeter, K., Wilson, L.B., Wallace, A., Hepburn, S., 2011. Transient and steady-state auditory gamma-band responses in first-degree relatives of people with autism spectrum disorder. Mol. Autism 2, 11. https://doi.org/10.1186/2040-2392-2-11.

Romeo, R.R., Choi, B., Gabard-Durnam, L.J., Wilkinson, C.L., Levin, A.R., Rowe, M.L., Tager-Flusberg, H., Nelson, C.A., 2021. Parental language input predicts Neuroscillatory patterns associated with language development in toddlers at risk of autism. J. Autism Dev. Disord. https://doi.org/10.1007/s10803-021-05024-6.

Ross, B., Herdman, A.T., Pantev, C., 2005. Right hemispheric laterality of human 40 Hz auditory steady-state responses. Cereb. Cortex 15, 2029–2039. https://doi.org/10.1093/cercor/bhi078.

Rubenstein, J.L.R., Merzenich, M.M., 2003. Model of autism: increased ratio of excitation / inhibition in key neural systems. Genes Brain Behav. 2, 255–267. https://doi.org/10.1034/j.1601-183x.2003.00037.x.

Seymour, R.A., Rippon, G., Gooding-Williams, G., Sowman, P.F., Kessler, K., 2020. Reduced auditory steady state responses in autism spectrum disorder. Mol. Autism 11, 56. https://doi.org/10.1186/s13229-020-00357-y.

Sivarao, D.V., Chen, P., Senapati, A., Yang, Y., Fernandes, A., Benitex, Y., Whiterock, V., Li, Y.-W., Ahlijanian, M.K., 2016. 40 Hz auditory steady-state response is a Pharmacodynamic biomarker for cortical NMDA receptors. Neuropsychopharmacology 41, 2232–2240. https://doi.org/10.1038/npp.2016.17.

Snijders, T.M., Milivojevic, B., Kemner, C., 2013. Atypical excitation-inhibition balance in autism captured by the gamma response to contextual modulation. NeuroImage: Clinical 3, 65–72. https://doi.org/10.1016/j.nicl.2013.06.015.

Sohal, V.S., Rubenstein, J.L.R., 2019. Excitation-inhibition balance as a framework for investigating mechanisms of neuropsychiatric disorders. Mol. Psychiatry 24, 1248–1257. https://doi.org/10.1038/s41380-019-0426-0.

Stapells, D.R., Galambos, R., Costello, J.A., Makeig, S., 1988. Inconsistency of auditory middle latency and steady-state responses in infants. Electroencephalogr. Clin. Neurophysiol. 71, 289–295. https://doi.org/10.1016/0168-5597(88)90029-9.

Stroganova, T.A., Komarov, K.S., Sysoeva, O.V., Goiaeva, D.E., Obukhova, T.S., Ovsiannikova, T.M., Prokofyev, A.O., Orekhova, E.V., 2020. Left hemispheric deficit in the sustained neuromagnetic response to periodic click trains in children with ASD. Mol. Autism 11, 100. https://doi.org/10.1186/s13229-020-00408-4.

Tadel, F., Baillet, S., Mosher, J.C., Pantazis, D., Leahy, R.M., 2011. Brainstorm: a user-friendly application for MEG / EEG analysis. Comput. Intellig. Neurosci. 2011, 1–9. https://doi.org/10.1155/2011/879716.

Tager-Flusberg, H., 2016. Risk factors associated with language in autism spectrum disorder: clues to underlying mechanisms. J. Speech Lang. Hear. Res. 59, 143–154. https://doi.org/10.1044/2015_JSLHR-L-15-0146.

Tager-Flusberg, H., Kasari, K., 2013. Minimally verbal school-aged children with autism Spectrum disorder: the neglected end of the Spectrum. Autism Res. 6, 468–478. https://doi.org/10.1002/aur.1329.

Takeshita, K., Nagamine, T., Thuy, D.H.D., Satow, T., Matsuhashi, M., Yamamoto, J., Takayama, M., Fujiwara, N., Shibasaki, H., 2002. Maturational change of parallel auditory processing in school-aged children revealed by simultaneous recording of magnetic and electric cortical responses. Clin. Neurophysiol. 113, 1470–1484. https://doi.org/10.1016/S1388-2457(02)00202-X.

Tan, H.-R.M., Gross, J., Uhlhaas, P.J., 2015. MEG-measured auditory steady-state oscillations show high test-retest reliability: a sensor and source-space analysis. NeuroImage 122, 417–426. https://doi.org/10.1016/j.neuroimage.2015.07.055.

Tang, X., Jaenisch, R., Sur, M., 2021. The role of GABAergic signalling in neurodevelopmental disorders. Nat. Rev. Neurosci. 22, 290–307. https://doi.org/10.1038/s41583-021-00443-x.

Taulu, S., Simola, J., 2006. Spatiotemporal signal space separation method for rejecting nearby interference in MEG measurements. Phys. Med. Biol. 51, 1759–1768. https://doi.org/10.1088/0031-9155/51/7/008.

Wechsler, D., 1991. The Wechsler Intelligence Scale for Children, Third edition. The Psychological Corporation.

Wickham, H., 2016. ggplot 2: Elegant Graphics for Data Analysis. Springer-Verlag, New York.

Wilkinson, C.L., Nelson, C.A., 2021. Increased aperiodic gamma power on young boys with fragile X syndrome is associated with better language ability. Mol. Autism 12, 17. https://doi.org/10.1186/s13229-021-00425-x.

Wilkinson, C.L., Levin, A.R., Gabard-Durnam, L.J., Tager-Flusberg, H., Nelson, C.A., 2019. Reduced frontal gamma power at 24 months is associated with better expressive language in toddlers at risk for autism. Autism Res. 12, 1211–1224. https://doi.org/10.1002/aur.2131.

Williams, K., Pinto, J., Irwin, D., Jones, D., Murphy, K., 2009. Age-related changes in the inhibitory : excitatory balance in macaque monkey primary visual cortex. J. Vis. 9, 1070. https://doi.org/10.1167/9.8.1070.

Williams, Z.J., He, J.L., Cascio, C.J., Woynaroski, T.G., 2021a. A review of decreased sound tolerance in autism: definitions, phenomenology, and potential mechanisms. Neurosci. Biobehav. Rev. 121, 1–17. https://doi.org/10.1016/j.neubiorev.2020.11.030.

Williams, Z.J., Suzman, E., Woynaroski, T.G., 2021b. Prevalence of decreased sound tolerance (Hyperacusis) in individuals with autism spectrum disorder: a Meta-analysis. Ear Hear. 42, 1137–1150. https://doi.org/10.1097/AUD.0000000000001005.

Wilson, T.W., Rojas, D.C., Reite, M.L., Teale, P.D., Rogers, S.J., 2007. Children and adolescents with autism exhibit reduced MEG steady-state gamma responses. Biol. Psychiatry 62, 192–197. https://doi.org/10.1016/j.biopsych.2006.07.002.

World Health Organization, 2016. International Statistical Classification of Diseases and Related Health Problems: ICD-10, 5th ed. WHO Press, p. 1075.

Xu, G., Broadbelt, K.G., Haynes, R.L., Folkerth, R.D., Borenstein, N.S., Belliveau, R.A., Trachtenberg, F.L., Volpe, J.J., Kinney, H.C., 2011. Late development of the GABAergic system in the human cerebral cortex and white matter. J. Neuropathol. Exp. Neurol. 70, 841–858. https://doi.org/10.1097/NEN.0b013e31822f471c.

Yizhar, O., Fenno, L.E., Prigge, M., Schneider, F., Davidson, T.J., O'Shea, D.J., Sohal, V. S., Goshen, I., Finkelstein, J., Paz, J.T., Stehfest, K., Fudim, R., Ramakrishnan, C., Huguenard, J.R., Hegemann, P., Deisseroth, K., 2011. Neocortical excitation / inhibition balance in information processing and social dysfunction. Nature 477, 171–178. https://doi.org/10.1038/nature10360.

Zhang, Z., Jiao, Y.-Y., Sun, Q.-Q., 2011. Developmental maturation of excitation and inhibition balance in principal neurons across layers of somatosensory cortex. Neuroscience 174, 10–25. https://doi.org/10.1016/j.neuroscience.2010.11.045.

Zikopoulos, B., Barbas, H., 2013. Altered neural connectivity in excitatory and inhibitory cortical circuits in autism. Front. Hum. Neurosci. 7, 609. https://doi.org/10.3389/fnhum.2013.00609.